



UNIVERSITY OF NAIROBI

Determination of the Effects of the Thermal Enhancement Process on Gemstones using X-Ray Diffraction and Raman Spectroscopy

Njogu, Sally Wangari

S56/78903/2015


University of Nairobi

A thesis submitted in partial fulfilment for the degree of Master of Science in Nuclear Science in the Institute of Nuclear Science and Technology in the University of Nairobi

@2022

Declaration

This thesis is my original work and has not been presented for a degree in any other university.

Signature:..........

Date: ...03-03-2022.....

Ms. Sally Wangari Njogu (S56/78903/2015)

Supervisors' approval

This thesis has been submitted with our knowledge as university supervisors:

Professor M. J. Gatari
Institute of Nuclear Science and Technology
College of Architecture and Engineering
University of Nairobi, Kenya.

Signature..........

Date....10.March.2022.....

Professor C. M. Nyamai
College of Biological and Physical Sciences
Geology Department
University of Nairobi, Kenya.

Signature..........

Date...10thMarch 2022.....

Dedication

I dedicate this research to my family who have supported me through it all. Their patience and understanding is by no means short of heroic.

Acknowledgements

I would like to acknowledge my professors and supervisors, Professor Gatari and Professor Nyamai, from the University of Nairobi. They have not only greatly added value to this research, but have also supported me with materials and access to laboratories to finish this research.

I would also like to acknowledge Professor Giuliani from France, who helped me with research papers written by experts in the area of gem enhancement, that helped me compile this research and understand the gems in Kenya.

I also thank NACOSTI for the funding they provided that enabled me to complete these research.

I cannot forget the help that I have had from colleagues in the Institute of Nuclear Science University of Nairobi and those from KEBS, Ministry of mining, and Department of Physics in Chiromo Campus. The labs technical teams were extremely helpful in the compilation of this research.

Finally, I thank God, who I must say without his help I would not have completed this research.

Table of contents

Declaration	ii
Supervisors' approval	ii
Dedication	iii
Acknowledgements.....	iv
Table of contents.....	v
List of tables	viii
List of figures	ix
List of abbreviations	xi
Abstract	xii
CHAPTER 1	1
INTRODUCTION	1
1.1 Background.....	1
1.2 Problem Statement	2
1.3 Research objectives	2
1.3.1 General Objective.....	2
1.3.2 Specific Objectives.....	3
1.4 Significance of study.....	3
1.5 Scope of study.....	4
CHAPTER 2	5
LITERATURE REVIEW.....	5
2.1 The Local Geology of Taita-Taveta County, Kenya.....	5
2.2 Factors influencing a gems chemistry and mineralogy.....	9
2.3 Gem Characteristics	13
2.4 The origin of color of gem stones	14
2.5 Thermal enhancement of gemstones and its effects on the appearance and structure of the gem in relation to other methods of enhancement.....	17

2.6	Techniques used to examine changes after gem enhancement	19
CHAPTER 3	24
METHODOLOGY	24
3.1	Research Design.....	24
3.2	Sampling Location	25
3.3	Sampling.....	26
3.3.1	Sampling Techniques	26
3.3.2	Sample Selection	27
3.3.3	Sampled Specimen	27
3.3.4	Sample Preparation.....	28
3.4	Sample analysis.....	28
3.4.1	X-Ray Diffraction Powder method (XRDP).....	28
3.4.2	Laser Raman Spectroscopy.....	30
3.5	Data analysis	31
3.5.1	X-Ray Diffraction Powder method (XRDP).....	31
3.5.2	Laser Raman Spectroscopy.....	32
3.6	Thermal enhancement	32
CHAPTER 4	35
RESULTS AND DISCUSSION	35
4.1	Thermal Enhancement effects on color of the specified gem samples	35
4.2	Optimization of the thermal enhancement procedure for the specific gem samples	40
4.3	The Physical, Mineralogical, Chemical and Morphological effects of the thermal enhancement on the gems samples	40
4.3.1	The Physical effects of the thermal enhancement on the gems samples	40
4.3.2	The mineralogical and chemical effects of the thermal enhancement on the gems samples	42
4.3.3	The morphological effects of the thermal enhancement on the gems samples.....	45
4.4	Comparison of thermally enhancement gems from various parts of the Mozambique belt	

.....	47
CHAPTER 5	53
CONCLUSIONS AND RECOMMENDATIONS	53
5.1 Conclusions.....	53
5.2 Recommendations	54
REFERENCES	56
Appendix A	66
Appendix B.....	67
Appendix C	68
Appendix D	69

List of tables

Table 4.1: Color changes for the ruby samples as temperature increases with constant increase in time.	35
Table 4.2: Color changes for the sapphire samples as temperature increases with constant increase in time.	36
Table 4.3: Color changes for the amethyst samples as time increases with constant increase in temperature.....	37
Table 4.4: Color changes for the smoky quartz samples as time increases with constant increase in temperature.....	38
Table 4.5: Gems grading system	38
Table 4.6: Physical changes observed in gem samples after the thermal enhancement process.	42
Table 4.7: Similarities and Differences between thermally enhanced gem samples from Taita-Taveta in Kenya and enhanced gems of the Mozambique belt.....	47

List of figures

Figure 2.1: A geological map of Kenya showing the Mozambique belt segments, East Mozambique Belt Segment (EMBS), North East Mozambique Belt Segment (NEMBS), South West Mozambique Belt Segment (SWMBS) and North West Mozambique Belt Segment (NWMBS). Outlined is the study area located in EMBS subsection III	6
Figure 2.2: A modified geological map of Taita-Taveta showing the gem mining districts Kuranze and Kasigau and the occurrence of the ruby, sapphire and tsavorite deposits.	8
Figure 2.3: Pressure Temperature (PT) conditions for the formation of corundum in metamorphic deposits	12
Figure 2.4: The diffraction of X-Rays by equally spaced identical planes of atoms governed by Braggs law $n \lambda = 2d \sin \theta$	20
Figure 2.5: An X-Ray pattern of $Ni_{0.5} Zn_{0.5} Fe_2O_4$ nanopowder calcined at 450 °C by EDTA method, (b) $Ni_{0.5} Zn_{0.5} Fe_2O_4$ nanopowder calcined at 850 °C by oxalate method.	21
Figure 3.1: A flowchart outlining the research design	24
Figure 3.2: Sample collection areas in Taita-Taveta County.	26
Figure 3.3: A 3.2 cm quartz gem quality sample (Grade A) Amethyst available in Taveta mines	28
Figure 3.4: A D8- Bruker X-Ray Diffractometer	29
Figure 3.5: The STR250 Laser Raman spectrometer	30
Figure 3.6: Thermal enhancement using the muffle furnace in Kenya Bureau of Standards (KEBS).	33
Figure 4.1: a) A graph showing temperatures ($^{\circ}C$) against color change for the ruby gem. b) A graph showing temperatures ($^{\circ}C$) against time for the ruby gem.	35
Figure 4.2: a) A graph showing temperatures ($^{\circ}C$) against color change for the sapphire gem. b) A graph showing temperatures ($^{\circ}C$) against time for the sapphire gem.	36
Figure 4.3: a) A graph showing temperatures ($^{\circ}C$) against color change for the amethyst gem. b) A graph showing temperatures ($^{\circ}C$) against time for the amethyst gem.	37
Figure 4.4: a) A graph showing temperatures ($^{\circ}C$) against color change for the smoky quartz sample. b) A graph showing temperatures ($^{\circ}C$) against time for the smoky quartz sample.	38
Figure 4.5: Photos showing raw and heated gemstones	41
Figure 4.6: Raman spectra of a corundum sample before thermal enhancement (λ excitation = 532 and 780 nm, processed, un-oriented).	43
Figure 4.7: Raman spectra of ruby sample gem after thermal enhancement (λ excitation = 514.5	

nm, processed, un-oriented).	43
Figure 4.8: Raman spectra of sapphire sample gem after thermal enhancement (λ excitation = 514.5 nm, processed, un-oriented).....	43
Figure 4.9: Raman spectra of a quartz sample before thermal enhancement (λ excitation = 532 and 780 nm, processed, un-oriented).	44
Figure 4.10: Raman spectra of amethyst sample gem after thermal enhancement (λ excitation = 514.5 nm, processed, un-oriented).....	44
Figure 4.11: Raman spectra of smoky quartz sample after thermal enhancement (λ excitation = 514.5 nm, processed, un-oriented).....	44
Figure 4.12: X-Ray Diffraction spectra of corundum sample before and after thermal enhancement.....	46
Figure 4.13: X-Ray Diffraction spectra of quartz sample before and after thermal enhancement.	47

List of abbreviations

- AsLS- Asymmetric weighed least squared
- CalTech- California Institute of Technology
- C.S- Convenience Sampling Technique
- EDXRF – Energy Dispersive X-Ray Florescence
- EMBS- East Mozambique Belt System
- HVCG- High Valued Colored Gemstones
- I.M.M.T- Institute of Minerals and Materials Technology
- IR- Infra Red
- JCPDS- Joint Committee on Powder Diffraction Standards
- KEBS- Kenya Bureau of Standards
- LRM – Laser Raman Micro spectrometry
- Ma 1- Magmatic sentustricto deposits
- Ma 2- Magmatic metasomatic deposits
- Ma B.P- a geological abbreviation of time meaning mega annum before present. Mega annum is a Latin word meaning in a million years.
- Me 1- Metamorphic sentustricto deposits
- Me 2- Metamorphic metasomatic deposits
- NEMBS- North East Mozambique Belt System
- NWMBS- North West Mozambique Belt System
- PDF - Pair Distribution Function
- P.S- Purposive Sampling technique
- RRUFF- A database containing an entire set of high-quality spectrum data from well-characterized minerals, and is working on the technology to share this data with the rest of the globe.
- Se- Sedimentary deposits
- S.R.S- Simple Random Sampling technique
- SWMBS- South West Mozambique Belt System
- TTCIDP- Taita Taveta county integrated development plan
- XRDP - X-Ray diffraction powder method
- XRFS- X-Ray fluorescence spectrometry
- XRPS- X-Ray Photo electron spectrometry

Abstract

This study determined the effects of an optimized thermal enhancement process on the quality of the ruby, sapphire, amethyst, and smoky quartz gem samples from Taita-Taveta County in Kenya. The study sought to improve the quality of low-grade gems by enhancing their color, clarity, and luster and, in turn, improving their competitiveness in the gem market because; the quality of the more significant percentage of gems in Taita-Taveta are low- grade when compared to the high-grade gems in the global market. Thermal enhancement was done using a muffle furnace, a standard cost method that alters the primary molecular structure of the natural gem mineral, thus changing its optical properties. It, in turn, alters the color, luster, cleavage, reflectance, and transparency. When the gem impurities are exposed to heat, they react differently, changing the molecular bonding and hence the overall atomic structure of the gem. After enhancement, the mineralogical, chemical, and morphological changes were analyzed using the X-Ray Diffraction powder method and Raman Spectroscopy. The study established that there was a notable color change for each selected gem sample as temperature increased. The optimum temperature is the one where there is an expected change in color, enhanced clarity, the deepness of color, and reduction in zoning. The study established optimum temperatures for the selected gem samples at 1200⁰C for rubies and sapphires, 450-550⁰C for amethyst, and 600-650⁰C for smoky quartz. The changes in ruby and sapphire ranged from deepening of the color, improved luster, and enhanced clarity by removing some impurities and removal of secondary zoning colors. Amethyst and smoky quartz were changed in color to citrine. It also established that the above physical changes were caused by chemical changes in the gems after the thermal enhancement process. The crystal structure of the corundum and quartz samples remained the same even after heating. There were similarities and differences between the thermally enhanced gems of Taita-Taveta and those from other Mozambique belt areas. The thermal enhancement process improved the low-quality gemstones and thus moving them to a different grade. Therefore, it is recommended that thermal enhancement be used to improve the quality of gems in Taita-Taveta at a large scale level. Further research should also be carried out with modern instruments for thermal enhancement and analytical methods for quantification.

CHAPTER 1

INTRODUCTION

1.1 Background

Recent accounts on Africa's potential concerning its gemstone production have emphasized the significance of the East Africa region in the gemstone market worldwide (Suleman, 1999; Simonet et al., 2000a). According to Giuliani et al. (2014a), Africa, in 2005, accounted for 90% of the world's ruby production, and Kenya accounted for 52%, Tanzania 28% and Madagascar 9%; 42% of sapphires; 33% of emerald and 100% of Tsavorite (Yager et al., 2008). In the past recent decades, Kenya and Tanzania have emerged as some of the topmost gemstone producers, despite their short gemstone mining history compared to other parts of the world such as Brazil or Sri Lanka (Simonet et al., 2000b). They are enriched with various colored gemstones like tanzanite, korerupine, scapolite, tsavorite, and tourmaline (Dirlam et al., 1992; Keller, 1992). The mining of gemstones and industrial minerals in Taita-Taveta has been ongoing for some years now. Current estimates indicate that the area is one of the leading gems produced in Kenya. (Kenya Engineer, 2010; TTCIDP, 2012).

Thermal enhancement has been practiced long since the 1900s' on various gems to improve their quality, and for a wide range of gem materials, it continues to be the most common enhancement method (McClure and Smith, 2000; McClure et al., 2010). Over the past two decades, heat treatment technologies such as electric furnaces with accurate pressure and temperature controls have become more accessible and sophisticated (Kammerling et al., 1990; McClure and Smith, 2000). Virtually all commercial heat treatment was carried out in Thailand during the 1980s and 1990s. Still, Sri Lanka has become a significant competitor in recent years. More minor yet effective thermal enhancements exist in other production regions like Myanmar, the U.S.A (in Montana), China, and Africa (McClure et al., 2010). In Kenya, small-scale miners have practiced thermal enhancement for some gem types, mainly trial-and-error processes. (Kievlenko, 2003).

The theoretical basis of this study is that the thermal enhancement process mimics the long geological processes that cause gemstones to be internally changed chemically, mineralogical, and structurally under heat and pressure conditions through magmatic processes, metamorphic processes, and hydrothermal fluid exchanges (Schwarz et al., 1996; McClure and Smith 2000). These internal changes then cause physical changes in the gem's color, luster, and clarity. The above theory is coupled with some debates in the gem market about the heating of gems under

high temperatures and low temperatures. The primary concern is not with the enhancement but with the amorphous substances left behind after the process in very high temperatures; where some have argued it was a byproduct of heating (Peretti et al., 1995; Shigley et al., 2000a), while others thought it was left there intentionally (Chalain, 1995; Emmet, 1999). At low temperatures, some research suggests that the effects of heat treatment may not be identified by any known method in most cases (McClure and Smith, 2000). This study was based on the above theory showing that geological processes cause the natural gemstones of various mineralogy, chemistry, and structure to be of different colors. The optimized thermal enhancement process produced various colorations of gems even more diverse than the natural process. This study determined the thermal enhancement process's physical, mineralogical, chemical, and morphological effects using the X-Ray Diffraction Powder method and Raman Spectroscopy.

The effects of the thermal enhancement process on the mineralogy, chemistry, and morphology of the chosen gems are essential in helping us understand how to optimize the process. The optimization of the process involves control of change in the color, brightness, luster, zoning, crystal structure, and clarity of the gems using heat and high pressures. Although Kenyan gems are of diverse types and are in high demand in the gem market (Giuliani et al., 2014a), some of them are of low (grade C) to very low quality (grade D) (Lexi, 2002). The low-quality gems sell at meager prices in the gem market (Mghanga, 2011), and thermal enhancement is intended to improve the gems' grade and thus add their value in the market.

1.2 Problem Statement

Despite the abundance of gems in Taita Taveta, the quality of the more significant percentage of gems in the area is low- grade (C) to very low- grade (D) in comparison to the ones in the global market, which are of exceptionally high grade (A) and high grade (B) quality. Competition, therefore, becomes a significant challenge for these gems in the market.

In gemstones that have color, the beauty and purity of the color is the main determining factor of its quality, followed by clarity and, to a lesser extent, cut (Maxwell, 2002; Mghanga, 2011). Therefore, it is crucial to explore various methods of enhancing quality by improving the color and clarity of the Taita-Taveta gems.

1.3 Research objectives

1.3.1 General Objective

The primary objective is to determine the physical, mineralogical, chemical, and morphological

effects of an optimized thermal enhancement process on gems using the X-Ray Diffraction Powder method and Raman Spectroscopy.

1.3.2 Specific Objectives

The specific objectives are:

1. To evaluate how thermal enhancement affects the color of specific gems samples (ruby, sapphire, amethyst, smoky quartz) in the Taita-Taveta area by heating the gemstones at particular temperatures and pressures in an oxidizing environment.
2. To establish the optimum temperature at which each gem color changes in terms of permanence, brightness, deepness, or a different color.
3. To establish the thermal enhancement process's physical, mineralogical, chemical, and morphological effects on the gems samples using the XRD powder method and Raman Analysis.
4. To compare the (physical, mineralogical, chemical, and morphological) effects of thermally enhanced gems from Taita-Taveta to those from other areas in the Mozambique belt.

1.4 Significance of study

The thermal enhancement process or heat treatment is when heat is applied to a gem in a controlled environment to improve the gem's appearance in terms of color, clarity, and luster. In particular, the study determines the effects of the thermal enhancement process on the physical (color, clarity, and brightness), mineralogical (chemical composition), chemical (constitution of substances), and morphological (the form and crystal structure) properties of the Ruby, Sapphire, Amethyst, Smoky Quartz samples in Taita-Taveta County in Kenya.

The quality of colored gemstones and 50% of their value is accounted for by the gem's color (Mghanga, 2011). Thermal enhancement is one of the relatively cheap enhancement methods that has been used to enhance gems in the past and affects the color of the gem significantly. It also improves the durability, vibrancy, and vividness of the gemstone (McClure et al., 2010; Pardieu 2010b). Optimization of this method for particular gems in Kenya could help improve the quality of the gems on a large scale and thus improve their competitiveness in the gem market. The demand

for the supply of high-value colored gemstones(HVCG)- ruby, sapphire, tsavorite, tanzanite, dematoid, and spinel doubled between 2005 and 2013 (Giuliani et al., 2014a). The jewelry industry has become a multibillion-dollar company in the last decade (Salama, 2011). For example, the beryllium diffusion of ruby and sapphires, practiced in Madagascar, was done to improve the color and vividness of the gems. The value per gem went up to about 200% of its previous price (Emmet et al., 2003). The beryllium diffusion into corundum also made them more attractive and vibrant in color.

The purpose of this study is to optimize the thermal enhancement method for the Ruby, Sapphire, Amethyst, and Smoky quartz gem samples in Taita-Taveta County and determine the physical, chemical, mineralogical, and morphological changes of the gems after the thermal enhancement process using X-Ray Diffraction and Raman Spectroscopy methods of analysis.

This study provides valuable knowledge in the scientific fields of geology and gemology. To the best of our knowledge, it is the only study focused on the effects of the thermal enhancement process on gems in the Taita-Taveta area. It is expected to make available some knowledge on the thermal enhancement, geographic region, geology, geochemistry, and mineralogy of gems in the Taita-Taveta area. Therefore, it should be helpful to material for reference to researchers and other readers in general.

1.5 Scope of study

This study uses XRD and Raman Analysis to study the physical, mineralogical, chemical, and morphological effects of thermal enhancement on gems in Taita-Taveta County, Kenya. It is limited to particular gem samples and only conducted in Taita-Taveta County between February and April 2019. A random sampling of the gemstones was used in two central gem districts; the Kuranze-Kasigau and Mgama- Taita. 20 samples of 1.0 cm-3.5 cm smoky quartz, amethyst, rubies, and sapphires gems are collected at a depth of 0.5 m- 40 m.

CHAPTER 2

LITERATURE REVIEW

2.1 The Local Geology of Taita-Taveta County, Kenya

In Kenya, the richest mineral and gem wealth occurs in the Neo-proterozoic age of the medium to high-grade metamorphic rocks (Keller, 1992). It is along the Mozambique Belt that is approximately 250 and 325 kilometers in width. It then stretches from Southern Ethiopia, southwards for at least 5,000 kilometers through East Africa to Mozambique, the east coast of Africa (Nyamai et al., 2003). The Mozambique belt is also referred to as the East African Orogeny (Stern, 1994).

Taita-Taveta County in Kenya has one of the richest mineral deposits (Keller, 1992; Mghanga, 2011) and is geologically located within the Mozambique belt. These include gemstones and industrial minerals that have been investigated, determined, and exploited for several years now (Banarafa, 1984; Mghanga, 2011). From the 1940s to 2000s, the wealth of the region has been documented by different researchers, including Walsh (1960), Williams (1966), Shibata (1975), Pohl and Niedermayr, 1980), Key and Rop (1987), Key et al. (1989), Keller (1992), Simonet et al. (2000 a, b), Nyamai et al. (2003) and Giuliani et al. (2014 a, b).

The earliest geological work describes hypersthene labradorite rocks from south Taveta as rich in colored gemstones. In July 1902, E. Walker visited Taveta and reported on significant developments of garnets in the gneissose hills to the south of the Taveta (Walsh, 1960; DuBois and Walsh, 1970). In the 1980s and early 1990s, Pohl and Niedermayr (1980) and Keller (1992) described the abundance of gemstones in the area of Wadawida, recording over 250 varieties of gemstones in Taita-Taveta. The description included rubies, sapphires, garnets, opal, amethyst, chrysoprase, carnelian, aquamarine, emeralds, and others categorized as precious, semiprecious stones.

By 2005, Kenya had accounted for about 90% of all rubies, 42% sapphire, 33% emerald, and 100% Tsavorite production in Africa. (Yager et al., 2008; Giuliani et al., 2014b) Taita-Taveta area (Fig 2.1) has been studied and described in detail to have Kuranze-Kasigau group of metasediments occurring in the Tsavo - Voi Area located in the South-Eastern part of Kenya, that comprise of

lithologies like quartzite and marble; graphite, sillimanite, kyanite gneisses, and schist and amphibolite (Nyamai et al., 2003). These rock types host the Ushindi ruby deposits in the Kuranze area, the Twiga sapphire deposit, and the amethyst hydrothermal deposits near Kasigau in Taita-Taveta District (Simonet et al., 2000a and b).

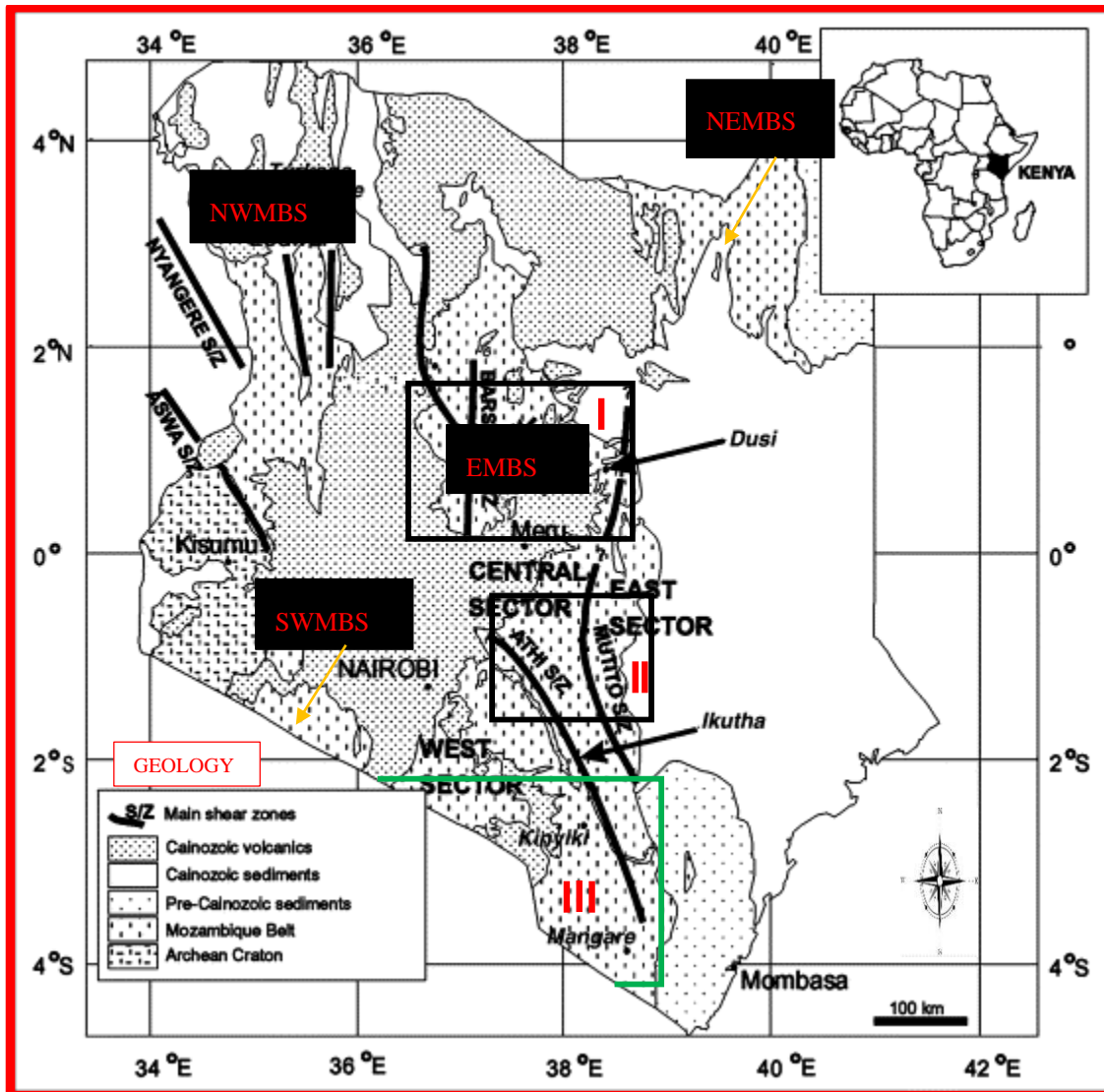


Figure 2.1: A geological map of Kenya showing the Mozambique belt segments, East Mozambique Belt Segment (EMBS), North East Mozambique Belt Segment (NEMBS), South West Mozambique Belt Segment (SWMBS) and North West Mozambique Belt Segment (NWMBS). Outlined is the study area located in EMBS subsection III (Adopted from Nyamai et al., 2003)

Geographically, the Taita-Taveta area lies in the East Mozambique Belt Segment (EMBS), between latitude 3°N and 4°S and longitude 37°E and 39°E. Specifically, in EMBS segment

III (Mosley, 1993; Nyamai et al., 2003), Figure 2.1 above. Determination of the gem's geographic location is one of the significant factors influencing the gem's mineralogy, geochemistry, and sale in the international market. The enhancement method is then chosen depending on the geochemistry, and expensive equipment is used to improve the discrimination of their origin (Giuliani et al., 2014a).

The stratigraphy of the rocks in the Taita-Taveta area fall into three main categories; the Archean rocks of the basement system (crystalline rocks), the tertiary volcanic, and the intrusive and superficial deposits of the Pleistocene and recent age. According to Nyamai et al. (2003), the geology of EMBS segment III is to a great extent similar to that of EMBS segment I but also with a notable difference in that it contains intertwined slices of ultramafic and mafic rocks with an ophiolitic nature that has undergone extreme deformation and very high-grade metamorphism in the mobile zone. According to Pohl and Niedermayr (1980), the Kurase unit shelf sequence rich in carbonates is separated from the overlying by an ophiolitic suture known as the Voi Suture Zone Kasigau unit and made of a monotonous sequence of meta-volcanic and metagreywackes (likely intruded by diorites).

There has been a significant increase in knowledge about the geochemistry of high-valued colored gemstones (HVCG) (Groat, 2007; Graham et al., 2008; Giuliani et al., 2011; Groat, 2012; Giuliani and Groat, 2012). Recently, the HVGC primary deposits have been put into three major subgroups: I.) the magmatic type (the corundum in alkali basalts and sapphires in lamprophyre and syenite), II.) metamorphic type (the corundum in the mafic and ultramafic rocks and marble, emeralds, tanzanites and tsavorite in quartz veins, tsavorite in nodule graphites and spinel in marble) and III.) the sedimentary type (emeralds deposits in lower cretaceous black shale) based on environments. (Simonet et al., 2000b; Giuliani et al., 2014a). In Taita-Taveta Area, we find rubies, sapphires, emeralds, garnets, including Tsavorite deposits, etc. (Simonet et al., 2001; Mghanga, 2011) in the above three environments.

The mineralogy of gems includes the physical properties, chemical composition, and the internal crystal structure of the gem, which the gems' occurrence or origin could influence in terms of physiochemical conditions (Simonet et al., 2002; O'Donoghue, 2006). The characterization and classification of gemstones into various categories is based on their hardness, color, refractive index, transparency, dispersion, fracture, cleavage, and luster. The four C's characterization of cut,

color, clarity, and carat has been used to grade diamonds and other minerals. For gemstones that contain color, the purity of the color and its beauty are the primary determinant of quality, followed by clarity then cut (Mghanga, 2011).

Figure 2.2 represents the relative occurrence of some of the most rewarding colored precious stones found in the Taita-Taveta area and the relationship between this occurrence and the geology. Although other varieties do exist in association with the ones below or separately, their value is very low.

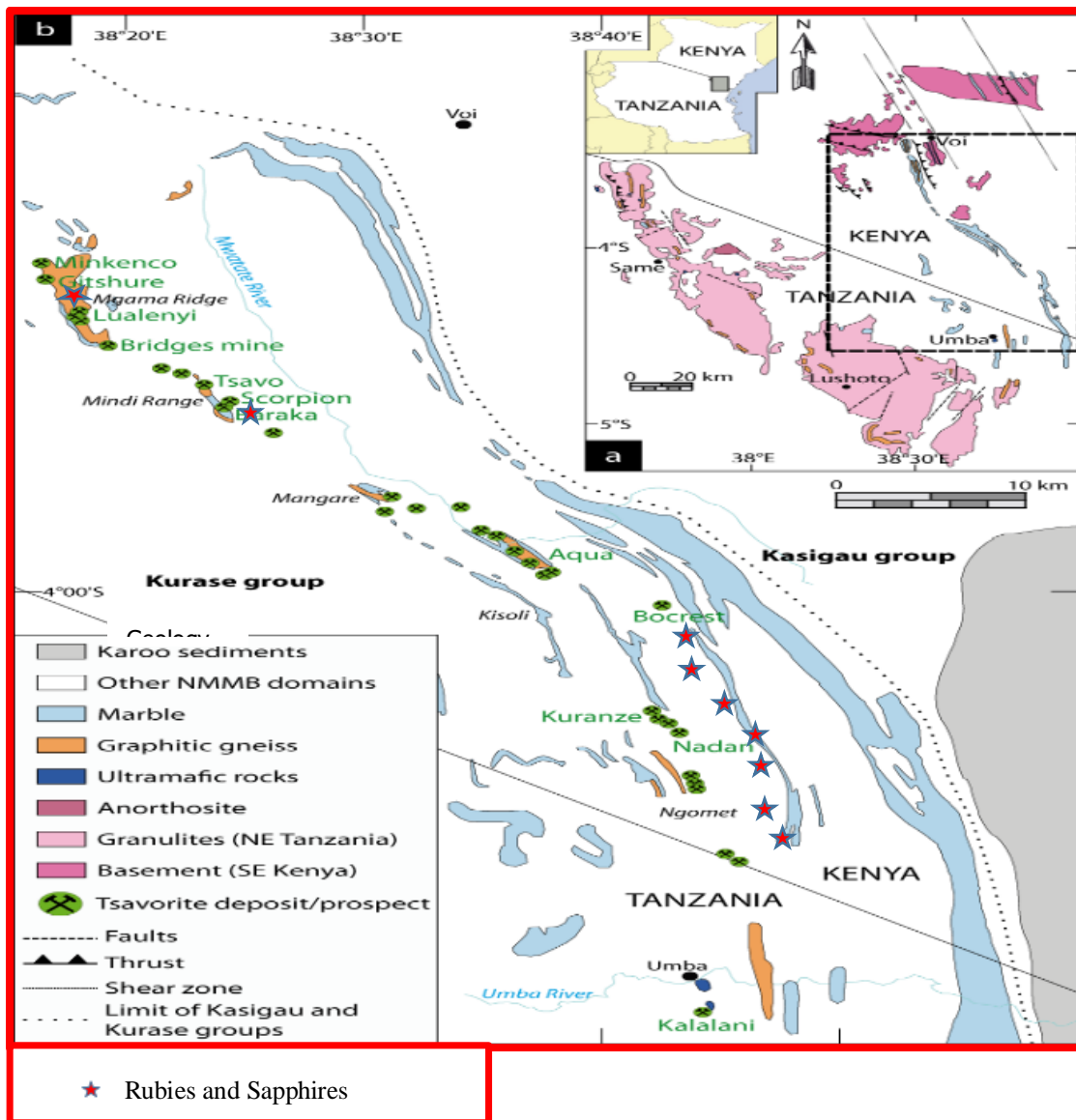


Figure 2.2: A modified geological map of Taita-Taveta showing the gem mining districts Kuranze and Kasigau and the occurrence of the ruby, sapphire and tsavorite deposits (Simonet, 2001; Giuliani et al., 2014b).

2.2 Factors influencing a gems chemistry and mineralogy

Corundum is said to belong to the hematite group (X_2O_3) of the rhombohedral oxides that consists of tistarite (Ti_2O_3), corundum (Al_2O_3), eskolaite (Cr_2O_3), hematite (Fe_2O_3), and karelianite (V_2O_3). According to Cesbron et al. (2002) and Giuliani et al. (2014b), no solid solutions are found between the five species above because they share the same structure. Quartz, however, is said to be a tectosilicate with the chemical formula of SiO_2 . It is trigonal, with each tetrahedron representing a SiO_4 - group. It comprises silica SiO_2 and some impurities of Al^{3+} , Li^+ , and Na^+ , haematite (Fe_2O_3) or magnetite (Fe_3O_4), and rutile (TiO_2) (Phillips and Griffen, 2004). The main factors influencing the above chemistry and mineralogy of a gem are these deposits' geology and formation processes.

Gemstones are encountered in a wide variety of rock types. Corundum, for instance, is a rare gem that can be hosted in different rock type but two major geological environments (Simonet et al., 2008), which are (1) amphibolite- to medium pressure granulite-facies metamorphic belts, e.g., in South Eastern Kenya and (2) alkaline basaltic volcanism in continental rifting environments. These are siliceous and mafic environments that are enriched in alumina and depleted in silica, but also contain Fe, Cr, and Ti that substitute for Al (Muhlmeister et al., 1998; Abduriyim and Kitawaki, 2006; Chitty, 2009) and have temperature and pressure conditions conducive for its stability and crystallization (Kievlenko 2003; Simonet et al., 2008). Corundum has a mineral association that mainly comprises sapphirine, biotite, plagioclase, phlogopite, pyroxene, carbonate, and amphibole minerals (Garnier et al., 2004). Rubies, for example, appear on bauxite soils during forest fires at atmospheric pressure (Simonet, 2008) and a high-pressure phase in diamonds (Watt et al., 1994).

Various geological and gemological literature have described the numerous and different gem localities worldwide (Simonet et al., 2002; Shigley et al., 2010). Their deposits around the world are found in different rock compositions, and thus the composition of the gems' composition varies in chemistry depending on the area of origin (Walton, 2004). The Mozambique belt has been known to be rich in both gemstones and industrial minerals. It is endowed with metamorphic rocks and intrusives. The belt has also been assumed to occur in several collisional sutures and superimposed Proterozoic subduction zones (Muhongo, 1998). It contains high-grade metamorphic rocks subjected to various electrothermal events between 845 and 715Ma B.P. (Cahen et al., 1984; Andressen et al., 1985).

According to Giuliani et al. (2014a), primary deposits are classified into three subgroups based on their magmatic, metamorphic, and sedimentary environments. Simonet et al. (2000a) and Giuliani et al. (2014b) divided the magmatic type into two, namely magmatic 1 and magmatic 2 (Ma 1 and Ma 2). Ma 1, the magmatic sentustricto deposits include corundum in the alkali basalts, sapphires in lamprophyre, and sapphires in syenite. In contrast, Ma 2, the magmatic- metasomatic deposits included the emeralds, rubies, alexandrite, and demantoid. The metamorphic type deposits were classified into Me 1 and Me 2. Me 1, the metamorphic sentustricto, included corundum in marble, mafic-ultramafic rocks, granulite and gneiss, tsavorite in nodule bearing graphite gneiss and spinel in marble (Hughes, 1997; Rankin, 2002). Me 2, the metamorphic- metasomatic related to fluid circulation in faults and shear zones crosscutting mainly metamorphosed shale and mafic-ultramafic rocks (less than 5% of sapphire deposits, 20% emerald deposits, tanzanite deposits (Cutten et al., 2003), and tsavorites in quartz veins) (Pardieu, 2007; Schwarz et al., 2008; Simonet et al., 2008; Chitty, 2009; Giuliani et al., 2014a). The sedimentary deposits (Se) included a particular case of Colombian emerald deposits located in lower cretaceous black shale and are related to the circulation of hydrothermal fluids in faults and shear zones.

The East African gem deposits have multiple geological similarities to those in other parts of the Mozambique Orogenic belt, namely, southern India, southern Madagascar, and Sri Lanka (Kroner, 1991; Olivier, 2006; Giuliani et al., 2007; Pardieu, 2010a). Many of the best-known sapphire deposits associated with metasomatized pegmatites closely relate to plumasites in East Africa occur in the Uмба area in Tanzania. In the Uмба Valley, a serpentinite plug was intruded by deposits of desilicified pegmatitic veins. The plug is securely surrounded by country-rocks composed of granulites, gneisses, and limestones. An anorthositic rock drained of silica and magnesia due to its contact with a serpentinite during emplacement is thought to have been the source of the pegmatite (Olivier, 2006). The hydrothermal processes caused the appearance of the plumasite rocks, which mainly contain corundum. (Chitty, 2009).

The geology of Tanzania is said to be a gradual slope from the Tanzanian Craton leading stepwise down to the Indian Ocean. These deposits were deposited by what could have been paleo river systems and generally lay to the north and northwest of Tunduru and were the primary cause of the deposition of rubies into the Tunduru area (Chitty, 2009). These rocks are collectively known as the Ubendian-Usagaran system of rocks. They produce almost every species of gemstones, most

evidently pyrope-almandine-spessartine garnets, tsavorite, ruby, alexandrite, tanzanite, emerald, uvite-dravite tourmalines, and sapphire (Cutten, 2002). These rocks also comprise multiple pegmatite intrusions, which are thought to assist in producing many gem species, inclusive of those gemstones that contain rare elements (Keller, 1992).

The Eastern Mozambique Belt segment (EMBS) contains one of the most abundant minerals deposits in the Eastern Africa region and Kenya. The corundum deposits field corresponds to a domain of temperatures between 500 and 800°C and pressures above 3 kbars. The lithologies are alumina rich and silica-deprived rocks like aluminous gneiss, marble, mafic and ultramafic rocks (M– U.M.) or felsic and silica-poor rocks such as limestone and marble that are influenced by fluid circulation at their contacts and changed by metasomatism (skarn, desilicated pegmatite, etc.) (Simonet et al., 2002; Giuliani, 2014b).

Figure 2.3 shows the pressure-temperature (P–T) conditions for the formation of corundum in metamorphic deposits in the P-T fields of North Carolina, Mangare, Morogoro, southern Kenya, Hunza, Sri Lanka, Greenland, Kashmir with three P-T boxes corresponding to the evolution of the fluids in the sapphire crystals from the center (c), to intermediate (i) and outer (o) zones, Urals, and Mong Hsu (Giuliani et al., 2014b).

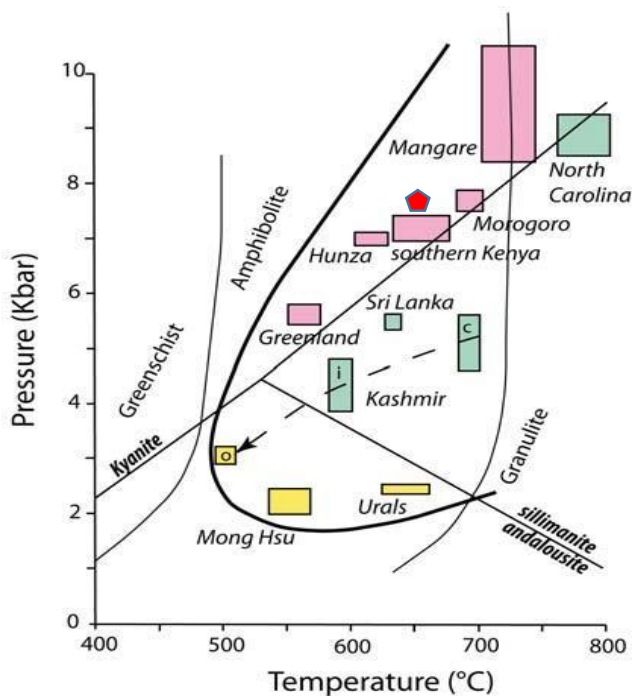


Figure 2.3: Pressure Temperature (PT) conditions for the formation of corundum in metamorphic deposits (Adopted from Simonet et al., 2008; Giuliani et al., 2014b).

Although it might be impossible to provide statistics for the world's colored stones mining districts, it is not that hard to confirm the significant areas and their relative importance. Sri Lanka (Ceylon), the Mogok area of Burma (Malisa and Muhongo, 1990), the Malagasy Republic Madagascar, Brazil (Dissanayake and Chandrajith, 1999), and, more recently, East Africa (Simonet et al., 2000b) are considered the most significant colored stone regions in the world, with every one of the areas producing several varied gemstones in reasonably large quantities.

According to Kroner (1984), the gemstone belt of Madagascar, Eastern Africa, Sri Lanka, and India was caused by the collision between the East and West Gondwana during the Pan-African tectometamorphic events. These events, therefore, explain why the primary sapphire and ruby deposits found in this gemstone belt are similar in geological age and chemistry. For example, southern Madagascar's metamorphic ruby and sapphire deposits, the eastern Africa deposits, the Sri Lanka deposits, and South Indian deposits have multiple geological similarities. (Rupasinghe

& Dissanayake, 1985; Silva & Siriwardena, 1988; Mercier et al., 1999a, b; Santosh & Collins, 2003; Giuliani et al., 2007; Rakotondrazafy et al., 2008; Dharmaratne et al., 2012; Feneyrol et al., 2013). John Paul Mine in Kenya has dated the geological age of formation of the protolith ruby–Pb in zircon from the Longido in Tanzania at 610 ± 0.6 Ma (Le Goff et al., 2010, John Saul mine in Kenya at 612 ± 6 Ma (Simonet, 2000c), and Vohibory deposits in Madagascar at 612 ± 5 Ma (Jöns & Schenk, 2008) showing a similar period of formation about the East African orogeny (Giuliani et al., 2014b).

2.3 Gem Characteristics

Various physical characteristics define a gem; the color of a gem, its hardness, density, luster, habit, cleavage, parting, and fracture, determined by the gem mineralogy, crystal structure, and chemistry.

QUARTZ

The most commonly occurring form of silica (SiO_2) is quartz. Quartz is diverse in color due to the type and level of impurities. Some colors are found in nature, but others can only be created in the laboratory. The colors range from colorless in pure quartz, to blue, white, red, pink, purple, yellow, green, brown, orange, black, grey, to multicolored. Quartz is vitreous in luster, has a hardness of 7 in the Mohr's scale, and has a hexagonal crystal structure, a specific gravity of 2.63- 2.65, a refractive index of 1.54-1.55, double refraction of 0.009, and an indiscernible cleavage (O'Donoghue, 2006). The gem quartz varies from amethyst and citrine to chalcedony, agate, carnelian and tiger's eye, chrysoprase, smoky quartz, pink quartz, ametrine, prasiolite, blue quartz, cats' eye, and tourmalinated quartz. Citrine is the most expensive and valuable market, followed by amethyst.

CORUNDUM

Corundum is made of aluminum oxide (Al_2O_3) in a colorless crystalline form when pure. Traces of different impurities such as titanium, chrome, vanadium, or iron are responsible for their color. Rubies have a variety of colors, from near colorless, to pink, to red, and then to a deep crimson. The rest of the colors are called sapphire with a color prefix. Rubies are the red variety of the corundum family that comprises aluminum oxide, chrome, and small proportions of other trace

elements – that depends on the occurrence of the gem. The color of ruby caused by the trace of chromic oxide (Cr_2O_3) comes into the crystal structure to a less extent by isomorphous replacement of the aluminum atoms. The amount of the trace replacement, about 1–3%, determines the depth of color. The presence of ferric iron modifies the tint by reducing fluorescence and gives, for example, the rubies from Thailand a characteristic brownish tint (O'Donoghue, 2006).

The red, pink, blue, yellow, or greenish sapphire is caused by small quantities of other elements, mostly iron and chrome, that alter the white crystals of pure corundum. The blue color in sapphire is caused by titanium and iron that have replaced aluminum in the corundum structure. Intervalence charge transfer involves $\text{Fe}^{2+} + \text{Ti}^{4+} > \text{Ti}^{3+} + \text{Ti}^{3+}$ (O'Donoghue, 2006), although evidence shows other possible causes for the blue color in sapphire.

Understanding the chemistry and characteristics of corundum is essential for anyone who wants to enhance its color by heating. Nassau (1996) established seven distinct ways in which the natural and artificial yellow sapphires could be colored; some procedures produced unstable colors, which could only be identified using a fade test to establish which stones were unstable. Fade testing is when a gemstone is subjected to light to try and weaken its color. It is used when a gemstone displays two colors, one that is a fading color and the other a non-fading color, and no other known test can distinguish between the two. One or more procedures can color yellow sapphire, and it may or may not always be possible to identify which process has colored a particular specimen in general testing.

2.4 The origin of color of gem stones

Gem enhancements are procedures applied to gems to improve appearance (which includes the color and clarity of a gem) and durability or, in some cases, the availability of that gem; for example, citrine can be made from heating amethyst at certain temperatures (McClure et al., 2010). Gem enhancement is considered permanent if the effects of the enhancement do not change under normal wear, when cutting, during repair, when cleaning, or on display. Most procedures involve the physics of light response to molecular structure (McClure and Smith, 2000; Winotai et al., 2014). Therefore, to fully apprehend the origin of color in gems, first, the researcher must understand the physics of light and, secondly, how this light interacts with the molecular and atomic structure of the gem.

At the turn of the 19th century, color became a major indication in identifying minerals. The simple correlation between a certain color and a particular element only works to some extent, and according to past research, several very varied processes can cause similar colorations (Nassau, 1983; Fritsch and Rossman, 1987). Gemstones are generally graded to categorize them into different price ranges in the gem market, and several characteristics have been used to categorize these gems (Lexi, 2002). Color can be influenced by external and internal factors, where the external factors influence how we perceive the coloration of the gem, while internal mechanisms cause color in gems (Pardieu et al., 2010a).

The external factors that influence our perception of the color of a gem to depend on two major factors: I.) the type of illumination and II.) the human eye. The gem's appearance depends on the light source, whether it's the sun, incandescent, or fluorescent (Kyi et al., 1999). An example would be alexandrite, which appears green in the fluorescent light and red in candlelight (incandescent light). This is because of the different spectral colors of the two light sources. The candle flame shows an orange tint because it emits more red, yellow, and orange than blue, which causes, for example, blue sapphires to appear almost black. Fluorescent light, however, emits larger proportions of light at the blue end of the visible spectrum, making it more desirable as a source of illumination for the blue-colored stones (Maxwell, 2002).

The human eye contains rods and cones, the light-sensitive cells in the retina. If the light intensity is dim, there is no color sensitization, and objects appear grey. The process is associated with rods, which contain only one pigment and are responsible for color in poor illumination. Color perception involves cones at higher levels of illumination. Each cone contains three fundamental pigments with maximum red, blue, and green absorption, respectively (Fritsch and Rossman, 1987). The human eye is always most sensitive to green and not equally sensitive to each visible color (Duplessis et al., 1985).

Internal factors causing color in gemstones are influenced by how the light interacts with the gemstone. Light entering the gem can be refracted, reflected, scattered, diffracted, transmitted, or absorbed. Absorption is the most important factor determining color, but several processes are possible. There are five main absorption causes, including I. dispersed metal ions (electrons of

transition metals or rare earth elements(REE)). II. Intervalence charge transfer. III. Color centers are also called Farbe or F- centers. IV. Bandgap colors and V. physical optics include scattering light, interference colors, and diffraction (Wang et al., 2006a).

The source of color is caused by the dispersed metal ions when the transition metal is either a major portion of the mineral chemistry or just an impurity (Hlava, 1990). The electrons of the transition metals are excited to open higher energy levels between a single ion's atomic orbitals, and this transition electron never leaves that central atom (Goivana et al., 2015). The electron, therefore, gains the necessary excitation energy by absorbing a particular energy or frequency (color) from the white light and thus causes the particular mineral to display the complementary color. Examples include; rubies, emeralds, and alexandrites (David and Fristch, 2001).

According to Fritsch and Rossman (1987) and Hlava (1990), intervalence charge transfers occurs when the valence electron from one atom absorbs just the right amount of energy(color) needed to make the transfer to the structure of an atom close by (often of a completely different element). Examples include; Fe^{2+} and Fe^{3+} of aquamarine and Fe^{2+} and Ti^{4+} of sapphires (Kane, 2008).

Color centers are created when atoms are oxidized or reduced (Hlava,1990). This occurs in nature due to radiation due to a universal occurrence of low concentrated natural radioactive isotopes of U, K, and Thor radiation in laboratories. After oxidation, a hole is left behind and is filled by an electron trying to substitute for the missing electron, and this electron comes from the adjacent atom. The unpaired electron left behind is inclined to absorb light energy of a certain frequency and create different unique colors. Examples include; in Smoky quartz, where Al^{3+} replaces a small part of Si^{4+} , and an amethyst, Fe^{3+} is changed to Fe^{4+} when irradiated (Goivana et al., 2015).

In bandgap theory, bandgap colors are produced by both semiconducting and insulating materials. For the bandgap colors to be produced, there must be an energy gap between the conduction and valence energy bands in the atom's electronic structure. The energy gap is clear, white, or an insulator if the material includes all wavelengths of light (Fritsch and Rossman, 1988b). The material is a semiconductor and colored if the band includes the energies part of the visible spectrum. For instance, in the case of cinnabar and diamond, it is an insulator where the bandgap is colored by impurities (Hlava, 1990).

Colors arising from the physical phenomenon, other than absorption, are caused by inclusions or lamellar texture. Diffraction, Interference, and scattering interact with the physical features to produce colors in gemstones (Wang et al., 2006b). Examples of the interference effect include; cracks in quartz. Examples of diffraction include; opal, labradorite, andradite (Nassau, 1983). While scattering effects include; fire opal, chrysoprase, and carnelian (Nassau, 1984).

2.5 Thermal enhancement of gemstones and its effects on the appearance and structure of the gem in relation to other methods of enhancement

Gem enhancement can be described as any process, besides fashioning, that improves the semblance or durability (Salama, 2011). There are different types of enhancement that include: dying, heating, stabilizing, diffusion, coating, bleaching, laser drilling, fracture filling, quench crackling, impregnation, and irradiation (Chalain, 1995; Peretti et al., 1995; McClure and Smith, 2000; Johnson and McClure, 2000; Shigley et al., 2000a, b; Wang et al., 2006b; McClure et al., 2010). However, the method of treatment chosen depends on the type of gem and the desired effect. Unlike the other enhancement methods, irradiation and heating in particular temperatures duplicate what happens in nature, thus indistinguishable from natural gem formation processes (Salama, 2011).

The first documented artificially irradiated gemstones were created by the English Chemist Sir William Crookes in 1905 when he buried diamond in powdered radium bromide. Still, commercial use has only been recently applied (Larsen et al., 2004). The most popular irradiation techniques are neutron and gamma irradiation from nuclear reactors. The gamma radiation from high-power Co-60 sources and charged elementary particles from accelerators are widely used for coloring and color enhancement of precious natural stones (Hall et al., 2000; McClure et al., 2010; Salama, 2011). This enables the production of gem colors that do not exist or those extremely rare in nature.

Irradiation enhances the optical properties of the gem, and high levels of ionizing radiation may alter the atomic structure of the gemstone's crystal lattice and, in turn, change the optical properties of the gem (Wang et al., 2005; Smith et al., 2008a, b and c). As a result, the gemstone's color is significantly altered, or the visibility of the inclusions lessened. Several operations may alter the color, and it is not always possible to pick out the specific process that has colored the specimen. Since some procedures produce unstable colors, only a fade test could be used to identify which

stones possessed that (Kammerling et al., 1990). The Institute of Minerals and Materials Technology (I.M.MT) in the U.S.A then observed color changes in red black rubies to light pink using microwaves of 3 MW and 150°C (Schmeltzer and Schwarz, 2007). Later, they used X-Ray fluorescence spectrometry (XRFS), Raman analysis, and X-Ray Photoelectron spectrometry (XRPS) to observe the changes of the untreated and treated gemstones. Black corundum, for example, is usually due to profuse inclusions. Fewer defects, irregularities, and impurities were due to changes in atomic structure (Johnson and McClure, 2000).

Salama (2011) summarized the effects of irradiated topaz by fast neutron irradiation in research reactors and gamma irradiation with a Co-60 source or inside cyclotrons. After the irradiation process, the color of the gemstones ranged from poor, to good, to excellent depending on the chemistry of the material, its place of origin (color centers), the irradiation technique, and the size of samples used (Nassau, 1983; Ashbaugh, 1988).

Previously, Cobalt-60 gamma rays were used to deliver a total dose of 10 mrad to 86 colorless topazes ($\text{Al}_2\text{SiO}_4(\text{FOH})_2$) samples at a dose rate of 0.7 mrad h^{-1} . The color produced was not uniform. Nassau (1985) later than recommended dose rates of less than 5 mrad h^{-1} to prevent an excessive build-up of the temperature inside the topaz during the process of gamma irradiation. The dose was also depended on the size of the sample and was recommended for any further studies that were to be carried out in the future of that field (Rossman, 1981; Ashbaugh, 1988; Ashbaugh, 1992).

Secondly, neutron bombardment was used on the colorless topaz samples. A deep, uniformly blue color was produced regardless of the size of the sample due to the excellent penetrating properties of neutrons. Unfortunately, this process produces radioactive by-products (McClure and Smith, 2000). Other studies show that fast neutrons that are $>1 \text{ MeV}$ produced the blue color while thermal neutrons that are $< 0.025 \text{ MeV}$ create the majority of radioactive isotopes in topaz (Jenkins and Larsen., 2004). The blue color was not correlated to dose in the case of neutron bombardment.

The comparison between the two methods shows that neutron bombardment produced a deeper blue color than in the gamma irradiation because neutrons induce more change to the crystal structure since they are more heavily ionizing and therefore penetrating the whole crystal (McClure and Smith, 2000; McClure et al., 2010). Each method, however, has its pros and cons. For example,

in the case of topaz, it took gamma irradiation nine months to induce homogenous coloration. In contrast, it took fast neutrons irradiation several hours to induce a similar coloration on the topaz sample (Salama, 2011). In the case of neutron bombardments, time is taken for the radionuclides formed to decay depending on their half-lives and activity to a value permissible for their application.

Although the methods mentioned above of enhancing gems have been variously used worldwide, one of the alternatives and cheapest methods of enhancement is the heating of gems. The heating of gems has been practiced ever since the 1900s, and though it requires little or no preparation of samples, little or no training for those experimenting, it is very efficient and has great results at the end of the process. Notably, this process is easily reversible in most cases and permanent in a few instances (Johnson and McClure, 2000). After being thermally enhanced, most of the gems return to their original color if exposed to certain light frequencies, and some are reversed by gamma irradiation (Winotai et al., 2004).

Heat treatment gems can sometimes be identified using routine gemological testing, but only very advanced laboratory instrumentation and techniques (Wang et al. 2006c; Shigley et al., 2008c; Shor and Weldon 2009). For others, heat treatment may not be distinguishable by any existing methods (Krzemnicki, 2010). Most gems like citrine, blue zircon, aquamarine, tanzanite have been treated over the years as a rule rather than an exception, but in most instances, someone cannot conclusively determine if the gems have been heat-treated or not. Heat-treated of corundum as a technique of gem enhancement has been used to generate or remove color, improve transparency by dissolving rutile inclusions, partially heal or fill surface cavities or fill surface-reaching fractures (Hughes and Galibert, 1998; Pardieu, 2010b)

2.6 Techniques used to examine changes after gem enhancement

X-Ray Diffraction powder method (XRDP) is an analytical method used for the most part to identify phases in crystalline materials and provides information on the unit cell dimensions of that material. It rapidly analyses the structure at the atomic and molecular levels to determine strain, preferred orientation, and grain size. On principle, any crystalline material is placed on a path of an X-Ray beam from a given source, and the X-Rays diffract through the crystal and into a detector. It is a widely used method as it measures the intensity of diffracted X-Rays at varying

angles to the incident beam, therefore, characterizing the crystalline phases within materials. The X-Ray Diffraction method measures and identifies both the number of minerals in a sample and identify phases (Hurai and Weirbicka, 2013).

The three-dimensional structure of crystalline materials, such as minerals, is defined by regular, repeating planes of atoms that form a crystal lattice. The interaction of a focused X-ray beam with these atomic planes causes part of the beam to be transmitted, another part absorbed, yet another refracted and scattered, and the rest diffracted. The diffraction of X-rays by a crystalline solid is similar to light by water droplets producing a rainbow (Wright, 2014). How each mineral diffracts the X-Rays is dependent on what atoms make up the crystal lattice of that mineral and how these atoms are arranged. A diffracted beam is produced when each diffraction beam produced by the planes is reinforced by another plane below it due to the regular stacking of the planes (Figure 2.4). Thus a diffracted beam results when the path difference between reflections from identical planes is equal to a whole number of wavelengths of the X-Rays in use.

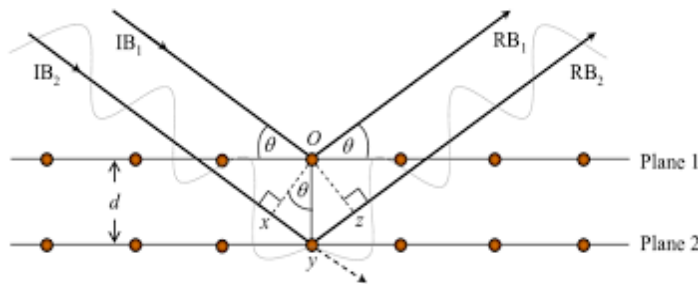


Figure 2.4: The diffraction of X-Rays by equally spaced identical planes of atoms governed by Bragg's law $n \lambda = 2d \sin \theta$. (Thomas, 2006)

The path difference between IB_1ORB_1 and IB_2YRB_2 is XYZ . $XY + YZ = 2d \sin \theta$ where d represents the inter-planar spacing between regularly spaced identical planes and is the glancing angle because it is the angle formed by an incident beam and the surface it strikes. Thus, a diffracted beam follows the direction ORB_1 or YRB_2

$$\text{Therefore, } n \lambda = 2d \sin \theta$$

The relationship $n \lambda = 2d \sin \theta$ is known as Bragg's Law. Where n is an integer signifying the order of the beam diffracted, λ is the wavelength of the incident X-ray beam, d is the distance between

adjacent planes of atoms (the d-spacing), and θ is the angle of incidence of the X-ray beam. The wavelength λ is known, and the angle of incidence θ can be measured. Therefore, the d spacing d can be calculated. The X-ray Scan generates a characteristic set of d-spacings that provide the unique identity of the mineral or minerals present in the sample. It is properly interpreted and compared with standard reference patterns and measurements, making it possible to identify the material.

In the X-Ray pattern of a calcinated NZF ($\text{Ni}_{0.5}\text{Zn}_{0.5}\text{Fe}_2\text{O}_4$) powders from the PDF database, the presence of the peaks at $2\theta = 18.50^\circ, 30.10^\circ, 35.5^\circ, 36.1^\circ, 43.3^\circ, 53^\circ, 57.3^\circ,$ and 62 corresponded to (111), (311), (220), (222), (422), (400), (440) and (511) diffraction planes (Figure 2.5) and confirmed the formation of a single-phase NZF, with a spinel structure. The low peaks indicated a low volume fraction of the NZF powder, while high peaks indicated a high volume fraction (Narenda et al., 2011).

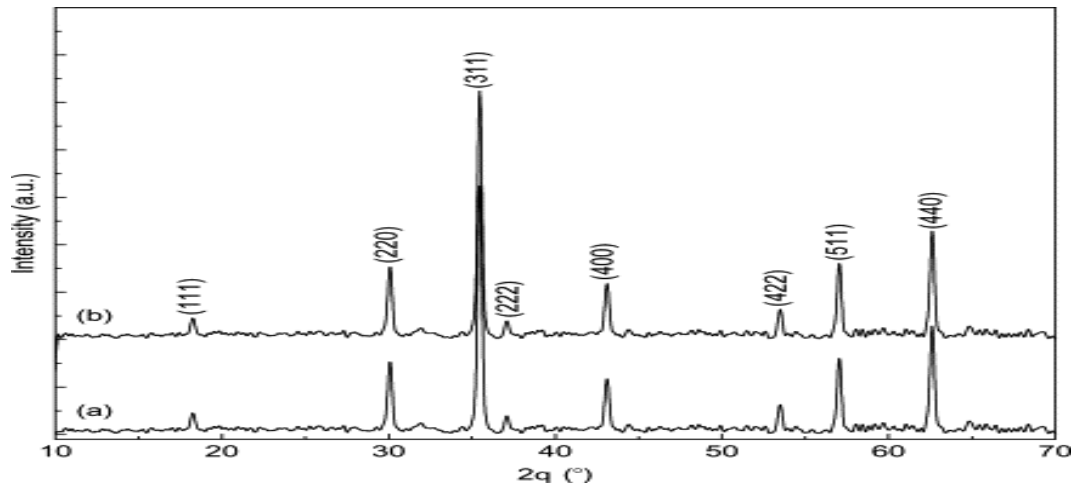


Figure 2.5: An X-Ray pattern of $\text{Ni}_{0.5}\text{Zn}_{0.5}\text{Fe}_2\text{O}_4$ nanopowder calcined at 450°C by EDTA method, (b) $\text{Ni}_{0.5}\text{Zn}_{0.5}\text{Fe}_2\text{O}_4$ nanopowder calcined at 850°C by oxalate method (Narenda et al., 2011).

Besides being a reliable and fast tool as a standard procedure for mineral identification, XRDP can provide additional information to determine the degree of crystallinity of the mineral(s) present. Someone can use it also to get the proportion of the different minerals present in a mixture and the degree of hydration in minerals that contain water in their structure. The presence of element

substitutions and solid solutions causes possible deviations of the minerals from their ideal compositions, the mineralogical structure (which can be used to deduce pressures and (or) temperatures of formation) (CalTech, 2009).

V. C. Raman discovered Raman scattering (or the Raman effect) in 1928, who later won the Nobel prize for his work. Raman spectroscopy is the study of matter by the inelastic scattering of monochromatic light, which involves the study of transitions between quantum levels of matter and molecules. Over the years, it has become a widespread tool in geochemistry, modern spectroscopy, microscopy, biophysics, and analytical chemistry (Herzberg, 1991).

Raman spectroscopy is advantageous because it is non-destructive and the lack of sample preparations involved, making it an ideal method for examining marketable gemstones (Jenkins and Larsen, 2004). There is the freedom to choose an incident wavelength that the surrounding media cannot absorb (useful for mineral or aqueous samples with strong IR absorption bands). Someone can also probe small volumes (the light can be focused to spots as small as micron-sized). The symmetry-based selection rules allow transitions that are not optically absorbed to be detected in scattering. However, it is disadvantageous in that it is less sensitive than emission or absorption spectroscopies because of the intrinsic weakness of the scattering process (Carey, 1982). When the incident light and a strong electronic transition in the molecule resonate, the Raman scattering signal greatly enhances. Low concentrations of inclusions in gems are detected due to the method's high sensitivity (Harris et al., 1990).

Suppose a material or substance is illuminated using a laser (monochromatic light). In that case, the scattered light spectrum is comprised of both a strong line (the exciting line) of the same frequency as the incident light and weaker lines on either side of the strong line shifted by frequencies ranging from about 100 to 3500 cm^{-1} . Those lines with a frequency less than the exciting line are known as Stokes lines, and the others with frequencies greater than the exciting line are known as anti-Stokes lines (Scmid and Dariz, 2019).

Typically, there is always be intense background associated with the fluorescence that accompanies Raman spectra and noise from the instrumental, environmental responses, and the physicochemical properties of the sample. There is, therefore, a need for the Raman spectra to be background corrected before chemical information can be properly extracted.

The key features of Raman band intensities could be elaborated using the simple classical electromagnetic field description (Laserna, 2006). The equation below shows how an external electric field, E , induces a dipole moment, P , proportional to the field in a molecule.

$$P = \alpha E$$

α is the proportionality constant that represents the polarizability of the molecule, and it quantifies how easily the electron cloud around a molecule can be distorted. The induced dipole scatters or emits light at the exact optical frequency of the incident light wave. According to Schmid and Dariz (2019), Raman scattering occurs because a molecular vibration induced by an external field changes the polarizability of the molecule.

Suppose any molecular vibration does not greatly change the polarizability, α . In that case, its derivative is near zero, like for the O-H bond, causing a low intensity of the Raman band. An external electric field, E , in such a case, may not induce any large changes in the dipole moment, P , and neither in the bending or stretching of the bond (Long, 2002).

Raman Spectroscopy can give information about the composition of material because each material has unique positions of each Raman peak, the intensity of the Raman peak shows the amount of material, the shifts in the frequency of peak intensities shows the stress/strain state, polarization of the Raman peak shows orientation and the crystal symmetry and the width of the Raman peak shows the quality of the crystal.

According to Schmeltzer and Schwarz (2007), X-Ray fluorescence spectrometry (XRFS), Raman analysis, and X-Ray Photoelectron spectrometry (XRPS) were used to observe the changes of the untreated and treated gemstones. The EDXRF (Energy Dispersive X-ray fluorescence) method was also used to determine the chemistry of the rubies from the Niassa area in Mozambique and the elements Cr, Ti, Fe, V, and Ga were analyzed. The quantitative data obtained about their chemistry can provide information regarding the source type and origin determination of different rubies and sapphires worldwide (Salama, 2011).

CHAPTER 3

METHODOLOGY

3.1 Research Design

An experimental research design is used in this study. Experimental research design systematically manipulates some characteristics and examines the outcome that holds all factors constant except the independent variable (Oso and Onen, 2009). It is used to test cause and effect relationships by manipulating variables in highly controlled settings.

Thermal enhancement is firstly done by the varying time of exposure while keeping gem chemistry and temperature constant, and secondly by varying temperatures while keeping gem chemistry and time of exposure. The XRD powder method and the Raman Spectroscopy are used to analyze the effects of the thermal enhancement on the gems under the above-stated conditions. Figure 3.1 is a flow chart diagram of the research design used for this study.

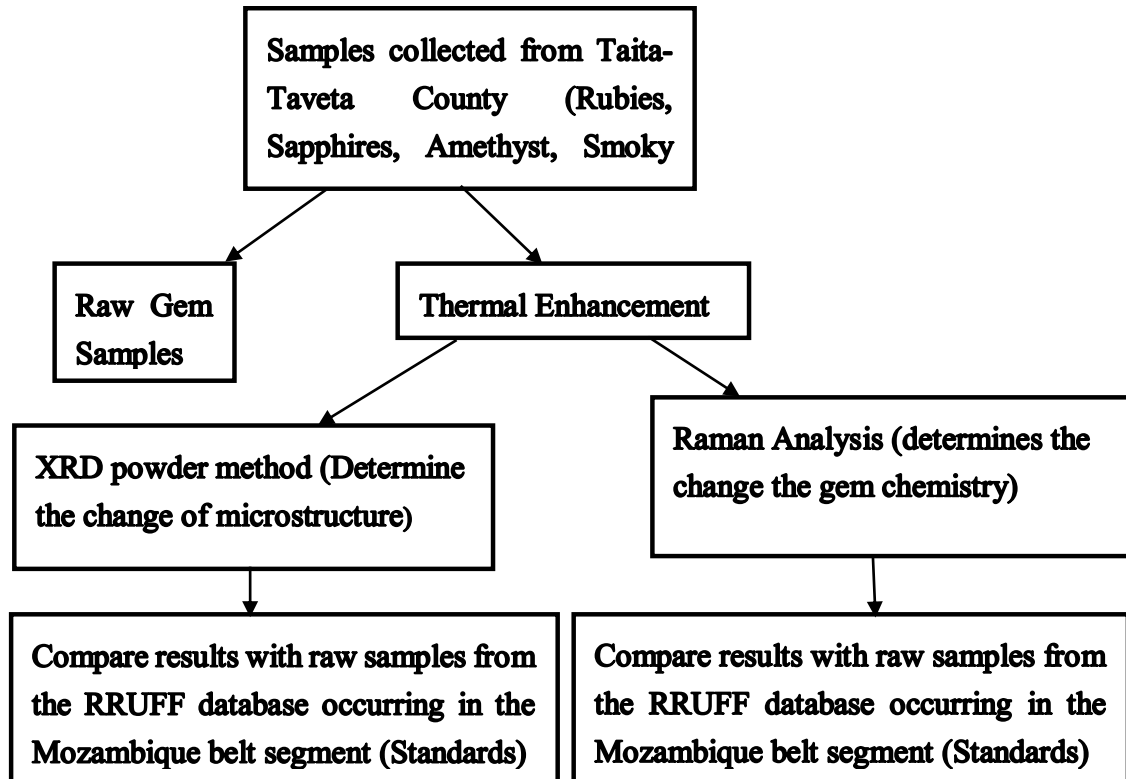


Figure 3.1: A flowchart outlining the research design

Observations are made on the change in physical appearances, optical properties, and atomic structure of the gems using the XRD diffraction method and Raman spectroscopy method. This design is selected because it is a sure way to establish the gems' mineralogical, chemical, and morphological changes after the thermal enhancement process.

3.2 Sampling Location

Taita-Taveta County was chosen for its richness in gem variety and availability in Kenya. It possesses the highest variety of exploitable gems in the rocks hosted by the Mozambique belt in Kenya, with about 200 species of gems, and its full potential is yet to be discovered. However, due to the constraints of inaccessibility, two major mining districts, the Kuranze-Kasigau and Mgama-Taita, have been chosen for this study. Figure 3.2 below is a map of Taita-Taveta county outlining the areas where samples were collected from.

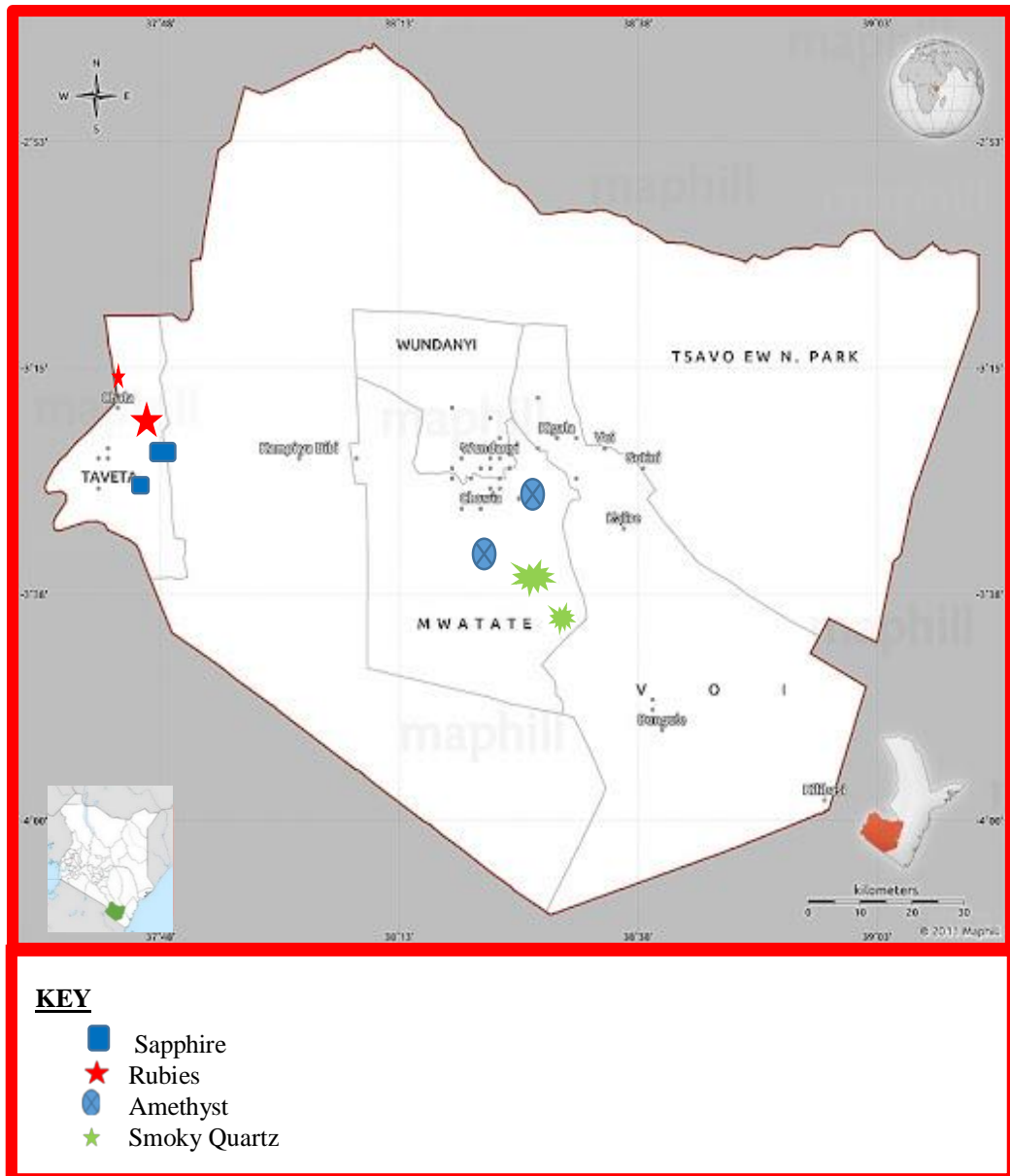


Figure 3.2: Sample collection areas in Taita-Taveta County. (Adopted from www.maphill.com)

3.3 Sampling

3.3.1 Sampling Techniques

This research employs three sampling methods: Simple random sampling, Purposive sampling, and Convenience sampling. Each sampling technique is carefully selected given the purpose, objectives, hypotheses, and variables in the research study.

Simple random sampling (S.R.S) refers to selecting a sample without any discrimination or bias

from the target population, mainly used to select a representative (random) sample. This research was used to select quartz and corundum samples from two major mining districts; Kasigau-Kuranze and Mgama-Taita. S.R.S is preferred in this study because any quartz or corundum gem from the study area has an independent and fair chance of being included in the samples collected.

Purposive sampling (P.S) refers to the researcher deciding on what characteristics to include in the samples collected based on typicality which means their specific characteristics. In this research, the purpose was to collect focused information on specific sizes of quartz and corundum samples ranging from 1cm-3.5cm and specific depths 0.5 m-20 m from four mines in Taita-Taveta County. This is useful because it saves time and sample collection costs.

Convenience sampling (C.S) is a technique that enables one to select a sample on a first-come, first-serve basis. This means the samples was to collect in real-time, and therefore it was the samples available at the time. Its purpose in this study was to collect available quartz and corundum samples from the mines on specific days of data collection. It is preferred in this research study because there is no rigidity of procedures, and it also helps in randomizing the sample population.

3.3.2 Sample Selection

The smoky quartz, amethyst, ruby, and sapphire gems were chosen for the experiment because; 1.) They are the most common (easily available) and varied minerals in Taita-Taveta. 2.) They fetch the highest prices in the market 3.) Their chemistry and atomic structure are also varied, giving better results variances.

A trained geologist or gemologist can use the above properties to ensure that other samples with similar characteristics, such as color, are not collected from sampling. However, for confirmation, the XRDP method was used as a redundancy to ensure only the correct samples were selected.

3.3.3 Sampled Specimen

The quartz samples (amethyst and smoky quartz), 10 in number, were collected from different depths ranging between 0.5 m to 40 m in the four different areas in Taita-Taveta (Fig 3.2). The size of the sample was between 1.0 cm and 3.5 cm. The quartz samples were of very low quality, grade D, cracked, and fresh and unaltered.



Figure 3.3: A 3.2 cm quartz gem quality sample (Grade A) Amethyst available in Taveta mines (Simonet et al., 2008).

Five rubies and five sapphires were collected from four areas in Taita-Taveta at depths of about 10-40m, as shown in Fig 3.2. Low to very low quality, grade three (C) and four (D) gems, respectively, were chosen from the areas in shear zones with their colors ranging from pink rubies and light blue sapphires.

The gem samples were packaged into different polythene bags for transport from the Taita Taveta Mines to the Kenya Bureau of Standards laboratory. Before analysis, they were stored in a dry and darkroom to avoid contamination and light exposure.

3.3.4 Sample Preparation

Samples were cleaned with dilute nitric acid to ensure removal of dirt and other impurities and half of them were then ground to a fine powder of less than 10 microns using a mill.

3.4 Sample analysis

3.4.1 X-Ray Diffraction Powder method (XRDP)

A D8- Bruker X-Ray Diffractometer from the Kenyan Ministry of mining and petroleum was used to perform the analysis. The Bruker XRD contains an X-Ray source of wavelengths of Cr, Co, Cu, Mo, and Ag, optics with high-intensity Ka 1,2 parallel beam and high-resolution Ka 1 parallel beam with a motorized divergent slit, a sample stage and specimen holder, a non-ambient chamber of temperatures ranging from 85K up to 2500 K, pressure of 10⁻⁴ mbar to 10 bar and humidity of 5% to 95% RH and a multi-mode detector with detection modes of 0D, 1D, and 2D based on hybrid photon counting technology. The D8 diffractometer contains a D8 ADVANCE and DIFFRACT.SUITE software allows it to support the simple execution of XRDP methods. It uses

positive material identification (PMI) with sensitivity to the atomic structure for phase identification. These methods include a semi qualitative analysis in EVA full pattern analysis in DIFFRAC.TOPAS and area methods in QUANT. A Voltage of 40 kilovolts is applied to accelerate the electrons, which then hit a target gem sample that has been ground to a fine powder (less than 10 microns), producing X-Rays. The detector measures the wavelength of these X-Rays characteristic of that particular gem.



Figure 3.4: A D8- Bruker X-Ray Diffractometer (Hurai and Weirbicka, 2013)

Procedure

1. A small sample was placed in the sample holder, and the surface of the sample was made smooth and compact to avoid large deviations between the peak intensities detected and the reference samples.
2. The sample holder containing the sample was placed in the XRD machine slot
3. The diffraction pattern of the sample was read, and the procedure was repeated twice for each gem sample.
4. The spectra were saved (on a memory disk) for analysis using TOPAS, MinCryst, and Excel software.
5. Comparisons between the gem sample spectrum and the online RRUFF database standard reference samples were made.

3.4.2 Laser Raman Spectroscopy

The STR250 Laser Raman spectrometer was used from the University of Nairobi, Chiromo Campus, Physics department. It contains a flexible, compact system that is highly sensitive to measure weak Raman scattering, a single MM or SM fiber, a remote probe for remote sampling, a high resolution of less than 1cm^{-1} . Grams/32 software used for advanced data processing, confocal optics for the microscope, and fully automated data collection. It also contains an imaging spectrometer. It contains an air-cooled Ar-ion laser source of 514.5 nm with the power of 100 mW being delivered to the sample at a high intensity that can produce Raman scattering with a high enough intensity to be measured compared to the background noise. The spectral acquisition was carried out using STR Raman spectrometer software (grams/32 by Seki Technotron Corporation, Japan). The spectrometer was directly coupled onto an Olympus BX 51 microscope with different objectives. A thermodynamically cooled CCD (Pixis 256, 1024 pixel by 256 pixels) is used for detection. The sample position placed on the microscope stage was computer-controlled in the XY direction, providing a point by point in the steps of 100 scanning. Being a confocal method, the depth profile can be estimated to be $2\ \mu\text{m}$. In this work, the raw spectra were background corrected using the Asymmetric Weighted Least –Squares (AsLS) followed by smoothing (using Savitzky Golay technique), both implemented in MCR-ALS GUI software.



Figure 3.5: The STR250 Laser Raman spectrometer (Laserna, 2006).

Procedure

1. The gem sample was placed into a sample compartment of the STR spectrometer, and the Raman spectrum was taken using grams/32 software.
2. The noise was corrected using the Asymmetric Weighted Least –Squares (AsLS) followed by smoothing (using Savitzky Golay technique), both implemented in MCR-ALS GUI software.
3. The spectra were saved and exported for analysis using Excel software.
4. Comparisons are made between the specific sample gems Raman spectrum and reference samples from the RRUFF database

3.5 Data analysis

3.5.1 X-Ray Diffraction Powder method (XRDP)

The XRDP D8 Bruker diffractometer contains a D8 ADVANCE and DIFFRACT.SUITE software that allows both crystalline and amorphous phases to be identified, texture or preferred orientation analysis, quantitative analysis of both crystalline and amorphous phase in mixtures of multiple phases. It is also used to determine specimen purity and microstructure analysis (disorder, crystallite size, microstrain, etc.), bulk residue stress that may result from thermal enhancement, indexing, crystal structure refinement, and initial crystal structure determination. The D8 ADVANCE and TOPAS software perform the Pair Distribution Function (PDF) analysis, an analytical technique that gives structural information from the disordered material based on diffuse and Bragg scattering. While Bragg scattering provides information about the average crystal structure of the material, diffuse scattering enables characterization of its local area structure.

Once the researcher has the Spectrum pattern, the procedure followed was assessing the background for amorphous scattering, background removal, peak finding, a compilation of the d values from peaks, and then comparison with the RRUFF database using search-match procedures for qualitative analysis. Once the researcher opens the JCPDS file, and selects the element used, for example, Cr₂O in the case of rubies and sapphires, then the PDF numbers were open in a new homepage. The researcher must select each PDF number and check whether the 100% peak matches the other two peaks (d-value). If it is, label the peak. Select each peak and check if it

matches the PDF number.

3.5.2 Laser Raman Spectroscopy

The STR250 laser Raman Spectrometer contains Grams/32 software for advanced data processing. The intense background associated with the fluorescence that accompanies Raman spectra and noise from the instrumental, environmental responses, and the physicochemical properties of the sample is corrected using the Asymmetric Weighted Least –Squares (AsLS). It is followed by smoothing (using Savitzky Golay technique), both implemented in MCR-ALS GUI software. There is a need for the Raman spectra to be background corrected before any chemical information can be properly extracted.

The corrected Raman spectrum gives us the composition of a material, each material having unique Raman peak positions. It also gives us the intensity of the Raman peak shows the amount of material on the X-axis. On the Y-axis, the pattern gives the shifts in the frequency of peak intensities that show the stress/strain state, polarization of the Raman peak, which indicates the orientation and the crystal symmetry, and the width of the Raman peak, which shows the quality of the crystal.

3.6 Thermal enhancement

Thermal enhancement is the process of heating gemstones in a controlled environment to alter their internal structures, and in this case, with a Muffle furnace that can go to a maximum temperature of 1200°C (Figure 3.4). The colors and other physical properties, therefore produced, depend on which procedure is used to get the best desired effects.



Figure 3.6: Thermal enhancement using the muffle furnace in Kenya Bureau of Standards (KEBS).

Muffle Furnace

The Muffle furnace used was an mrc series product (Figure 3.6) that uses a furnace material of vacuum-formed high purity alumina ceramic fiber. A high-quality alloy-resistant wire is used as a heating element. The temperature controller has a microcomputer PID control module that helps it attain precise temperature control and the constant temperature required. The heating rate is 0-10⁰C every min from room temperature to 1200⁰C. When the instrument program temperature is required and time is set, the sample gem is placed in the oven chamber, and the run button is pressed. The heating process is completely automated, and an alarm signal automatically switch off the oven after the time and temperatures set are reached.

Procedure

There was no sample preparation required, and the sample's integrity was preserved. Eight samples were chosen for this experiment, two for each gem, ruby, sapphire, amethyst, and smoky quartz. After cleaning with dilute nitric acid, each sample was put inside the Muffle Furnace. The temperature is then regulated from the range of 0 ⁰C-1200 ⁰C in an oxidizing environment for a period of 3-6 h, depending on the gem sample. Rubies were put in the Furnace for six h at temperatures between 800⁰C-1200⁰C. Color changes were observed every 15min, and

corresponding temperatures were recorded. Sapphires were put in the Furnace for five h at temperatures between 800⁰C-1200⁰C. Observations were made every 15minutes, and color changes were recorded. For smoky quartz and amethyst samples, the color change was observed after every 50⁰C rise in temperature from 250⁰C to 600⁰C for some time of 3 h and 4 h, respectively. The maximum temperatures reached were 1200⁰C, limiting the muffle furnace used.

With every change of color, there implies a change in each of the gems' molecular structure or chemistry. The above changes were analyzed using the X-Ray Diffraction powder method and Raman Analysis.

CHAPTER 4

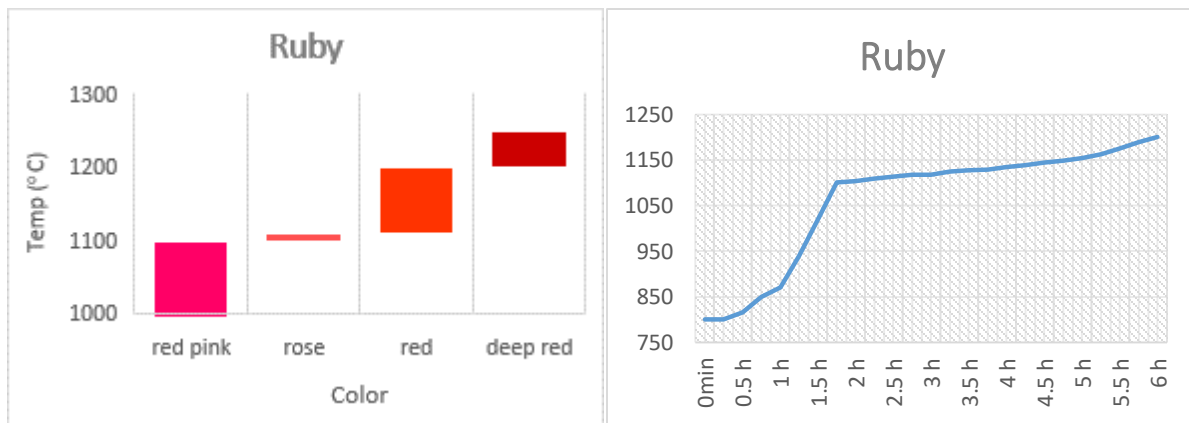
RESULTS AND DISCUSSION

4.1 Thermal Enhancement effects on color of the specified gem samples

The ruby was heated at a steady temperature of between 800⁰C-1200⁰C for 6 h and the color was recorded after every 0.25 h (Table 4.1 and Fig. 4.1). The color changed from red pink to rose red after 1.75 h at 1100⁰C, then to red after 1.5 h at 1124⁰C and to deep red 1.75 h later at 1200⁰C. The temperature 1200⁰C was kept constant for 1 h after that, but no change in color was observed.

Table 4.1: Color changes for the ruby samples as temperature increases with constant increase in time.

Time	Temperature (° C)	Color
0 h - 1.5 h	800-1020	Red pink
1.75 h – 3 h	1100-1120	Rose
3.25 h – 5 h	1130-1190	Red
5.25 h – 6 h	1200	Deep red



a)

b)

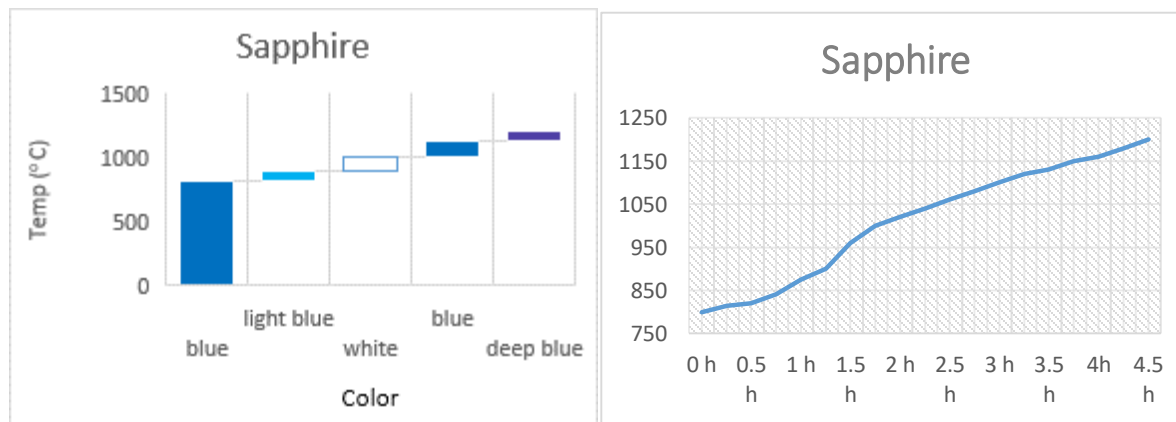
Figure 4.1: a) A graph showing temperatures (°C) against color change for the ruby gem. b) A graph showing temperatures (°C) against time for the ruby gem.

Sapphire was heated at a gradual increase in temperature of between 800⁰C-1200⁰C, for 5 h and

the color was recorded after every 0.25 h (Table 4.2 and Fig. 4.2). The color of the raw sample was blue. After heating for 1 h, it changed to light blue at 875⁰C. The color then changed to white at 1000⁰C, 0.75 h later. At 1100⁰C which was 1.25 h later, it changed to blue followed by deep blue after 2 h at 1200⁰C.

Table 4.2: Color changes for the sapphire samples as temperature increases with constant increase in time.

Time	Temperature (° C)	Color
0 h	800	Blue
0.25 h - 1 h	815-875	Light Blue
1. 25 h - 1.75 h	900-1000	White
2 h – 3 h	1020-1100	Blue
3.25 h - 5 h	1120-1200	Deep Blue



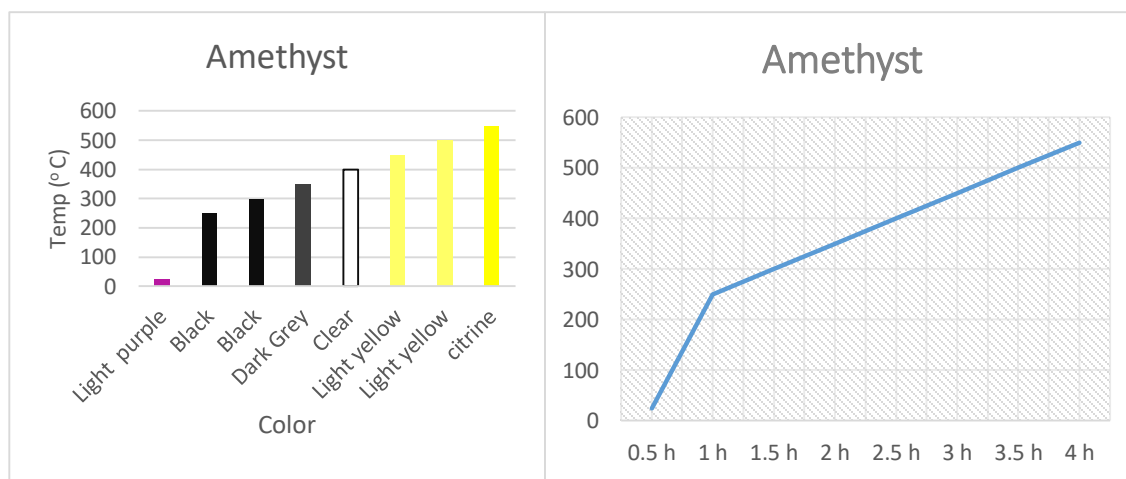
a) **Figure 4.2: a) A graph showing temperatures (°C) against color change for the sapphire gem. b) A graph showing temperatures (°C) against time for the sapphire gem.**

The amethyst sample was heated at 250⁰C to 600⁰C for 4 h and color change was recorded after every 50⁰C (Table 4.3 and Fig. 4.3). The color of the raw sample was light purple. Having pre heated the oven for 1 h to 250⁰C, once placed inside, the sample instantly changed to black. It then changed to grey at 350⁰C after 1 h, and then to clear at 400⁰C after 0.5 h. At 450⁰C which was 0.5

h later, it changed to yellow which deepened between the temperatures of 500⁰C and 550⁰C after 1 h.

Table 4.3: Color changes for the amethyst samples as time increases with constant increase in temperature.

Time	Temperature (⁰ C)	Color
0.5 h	25	Light purple
1 h	250	Black
1.5 h	300	Black
2 h	350	Dark Grey
2.5 h	400	Clear
3 h	450	Light yellow
3.5 h	500	Light yellow
4 h	550	Citrine



a)

b)

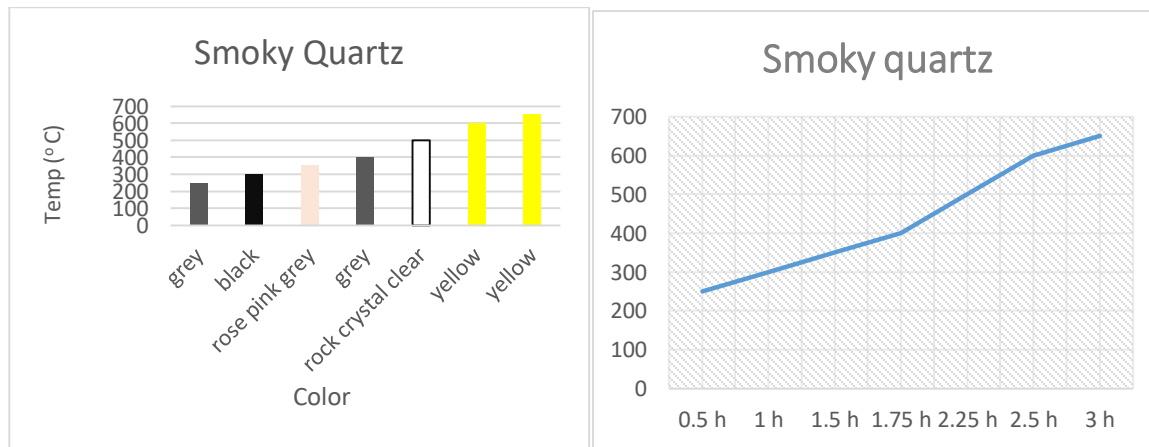
Figure 4.3: a) A graph showing temperatures (⁰C) against color change for the amethyst gem. b) A graph showing temperatures (⁰C) against time for the amethyst gem.

The smoky quartz sample was heated from 250⁰C to 600⁰C, for 3 h and color was recorded after every 50⁰C (Table 4.4 and Fig. 4.4). The color of the raw sample was light grey. After 1 h of heating it changed to black at the temperatures of 300⁰C. The color then changed to rose pink grey

at 350⁰C after 0.33 h and then to clear at 500⁰C after 1 h. At 600⁰C which was 0.5 h later, it changed to yellow. The yellow color deepened as temperature increased from 600⁰C to 650⁰C for 0.5 h.

Table 4.4: Color changes for the smoky quartz samples as time increases with constant increase in temperature.

Time	Temperature (⁰ C)	Color
0.5 h	250	Grey
1 h	300	Black
1.5 h	350	rose pink grey
1.75 h	400	Grey
2.25 h	500	rock crystal clear
2.5 h	600	Yellow
3 h	650	Yellow



a)

b)

Figure 4.4: a) A graph showing temperatures (⁰C) against color change for the smoky quartz sample. b) A graph showing temperatures (⁰C) against time for the smoky quartz sample.

Table 4.5: Gems grading system (Adopted from Lexi, 2002).

Grade	Hue and color saturation	Color tone	Inclusions	Transparency /opacity	Cutting
A	Color is the	Color tone	There are few,	Translucency/	Cutting or shape is

	hue expected. Color saturation is vivid and even throughout the stone.	is rich, but not so dark as to be near the far end of the spectrum.	if any, inclusions. Any inclusions are small and hard to spot with the naked eye.	Opacity is as expected for the specific stone.	uniform. Surface has a smooth luster, high polish and no cracks or chips. The drilling of the hole is even and uniform.
B	Color is the hue expected, but may not be as vivid as an A grade. Saturation is fairly even throughout the stone.	Color tone is good, but may be lighter or darker than an A grade stone.	A few inclusions are seen, but they are small and unobtrusive.	The stone may not have the clarity or opacity of the same stone in an A grade.	Cutting or shape may exhibit some slight variances. Surface has a medium luster and moderate polish, cracks or chips are minimal and drilling is generally uniform.
C	The color of the stone is within the hue expected, but may not be vivid or even.	Color tone is significantly lighter or darker--near the ends of the spectrum.	Inclusions or matrix mineral content is more apparent and frequent. These are easily visible to the naked eye.	The stone may vary greatly in clarity/opacity from that expected.	Cutting or shape exhibits some variances. Surface has a medium to low luster and polish. Cracks or chips are more apparent. Drilling may lack uniformity.
D	Color of the stone is generally the color expected, but saturation is low and very uneven.	Color tone can be so deep it seems black or so light it seems colorless.	Inclusions are frequent and greatly affect the overall look of the stone.	Stones expected to be transparent may be opaque or be heavily included. Stones expected to be opaque may have less original material and more "other" mineral content, causing more transparency.	Cutting or shape can be irregular. Surface has poor luster with cracks or chips. Drilling can be uneven.

4.2 Optimization of the thermal enhancement procedure for the specific gem samples

In this study, optimization of the thermal enhancement process is the temperature at which the gem color changes in terms of permanence, brightness, deepness or to a totally different color. The results of Fig. 4.1, 4.2, 4.3 and 4.4, indicate that as temperature increased, the color changed several times for each sample, till an optimum temperature or the maximum furnace capacity was reached. The ruby changed from rose pink to a deeper shade of red while sapphire turned from blue to a deeper blue. The Amethyst turned from purple to yellow (citrine) with the smoky quartz turning from dark grey to yellow (citrine).

The optimum temperatures for the gem samples was selected as 1200⁰C for ruby and sapphire after heating them for 6 h and 5 h respectively in an oxidized environment. For amethyst the optimum temperature was selected to be 450⁰C -550⁰C, after heating for 4 h in an oxidized environment and 500⁰C -650⁰C for smoky quartz after heating for 3 h in an oxidized environment. This means that at this temperature the sample gems showed the expected color changes (amethyst to citrine and smoky quartz to citrine) or brighter and deeper colors than the raw gems as in the case of the ruby and sapphire.

4.3 The Physical, Mineralogical, Chemical and Morphological effects of the thermal enhancement on the gems samples

4.3.1 The Physical effects of the thermal enhancement on the gems samples

After physical examination of the heated samples, some improved in color, where color deepened, lightened or changed. Figure 4.5 suggests some physical characteristics were altered in addition to the color changes after the gems were heated. At the top left – A1) a 1.2 cm diameter raw ruby sample and A2) a 1.2 cm diameter heated ruby sample, top right – B1) a 1.7cm diameter raw sapphire sample and B2) a 1.7 cm diameter heated sapphire sample, bottom left - C1) a 1.4 cm diameter raw amethyst sample and C2) fractured pieces 0.3- 0.8 cm diameter heated amethyst samples, bottom right – D1) a 1.6cm diameter raw smoky quartz sample and D2) a 1.3 cm diameter heated smoky quartz sample. There was removal of secondary colors and therefore reduction of color zoning. There was also development or removal of silk, therefore improving the luster of the gem and the clarity of the gem was enhanced. The results are summarized in the Table 4.5.



A₁ Raw Ruby sample

A₂ Heated ruby sample

B₁ Raw Sapphire sample

B₂ Heated sapphire sample



C₁ Raw Amethyst sample

C₂ Heated amethyst sample

D₁ Raw Smokey quartz sample

D₂ Heated smoky quartz sample

Figure 4.5: Photos showing raw and heated gemstones

The results in Table 4.6 below, indicate some of the physical changes that occurred in the gem samples after heating. These physical changes were determined by the type of gem enhanced, what temperatures were used to heat the particular gem sample and for how long. The changes in the corundum samples, ruby and sapphire, ranged from deepening of the color, improved luster, enhanced clarity of the gem by removal of some impurities and removal of secondary zoning colors. Amethyst and smoky quartz changed in color to yellow (citrine).

This deepening and changes in color for corundum samples are due to change in mineralogy and chemistry of the gem samples after heating. For the ruby sample (Al_2O_3), Al^{3+} is substituted by Cr^{3+} which causes the red color in rubies (Hughes, 1997). As for sapphires, Al_2O_3 contains impurities of Ti and Fe. It changes some of the Fe^{3+} ions into Fe^{2+} ions and then Ti^{3+} ions to Ti^{4+} ions (Smith et al., 1997). The balance between the two processes determines how deep or light the color.

For the amethyst gem and the smoky quartz, the thermal enhancement process is responsible for the color change caused by a color center in both. (See Appendix B- more information on chemical

ions responsible for color change in gems).

There were no observable undesirable effects of heating these gemstones at the particular temperatures chosen. This could be because the temperatures were not high enough to cause melting of the gemstones. The effects of enhancement were semi-permanent with fading been observed after a few days in samples that were exposed to direct sunlight. For those stored in a dark lit room and at room temperatures, the effects remained stable and permanent.

Table 4.6: Physical changes observed in gem samples after the thermal enhancement process.

GEM TYPE	COLOR CHANGE	CLARITY	LUSTER	COLOR ZONING
Rubies	Deepened the color	Enhanced	Development of silky luster	Little removal of purplish hue
Sapphires	Deepened the color	Enhanced	Development of silky luster	None
Amethyst	Amethyst changed to citrine	Enhanced	Vitreous luster	Development of a reddish tint
Smoky quartz	Smoky quartz changed to citrine	Enhanced	Vitreous luster	Development of a reddish tint

4.3.2 The mineralogical and chemical effects of the thermal enhancement on the gems samples

The gems mineralogy, chemistry and morphology were analyzed by Raman spectroscopy and X-Ray diffraction powder method. The results were then compared to reference samples from the RRUFF database. The results of the thermally enhanced gems are summarized in Figure 4.6, 4.7, 4.8, 4.9, 4.10, 4.11, 4.12 and 4.13.

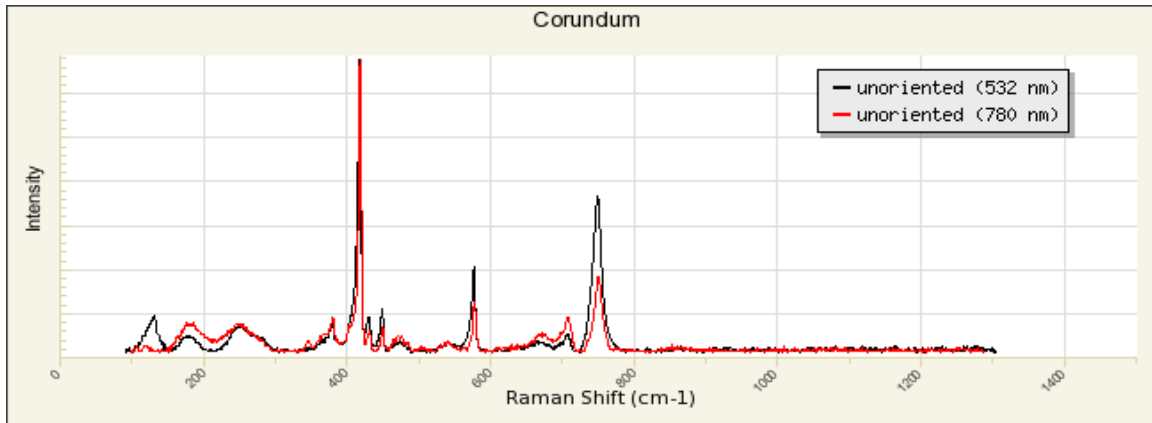


Figure 4.6: Raman spectra of a corundum sample before thermal enhancement (λ excitation = 532 and 780 nm, processed, un-oriented).

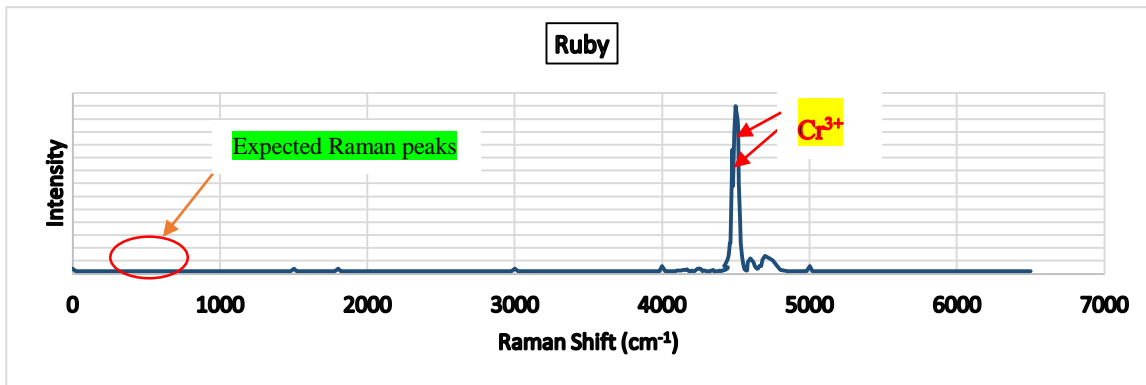


Figure 4.7: Raman spectra of ruby sample gem after thermal enhancement (λ excitation = 514.5 nm, processed, un-oriented).

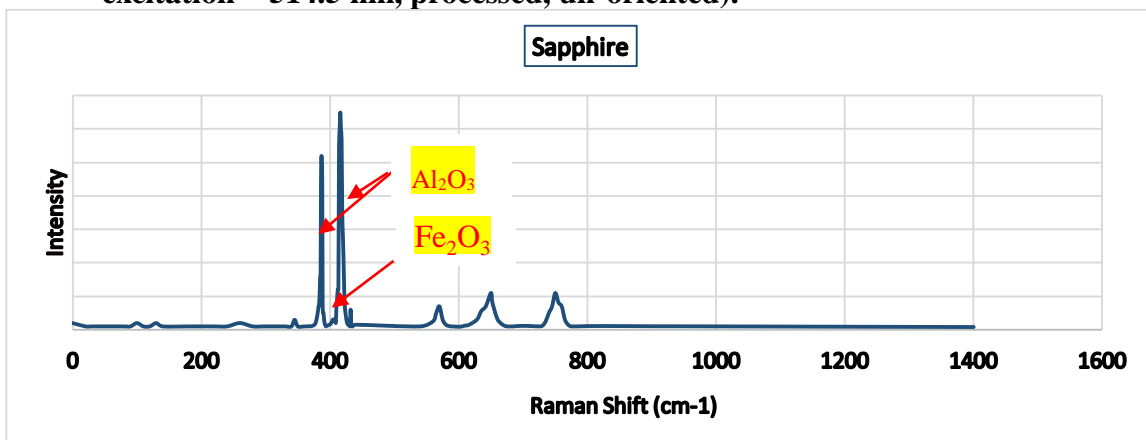


Figure 4.8: Raman spectra of sapphire sample gem after thermal enhancement (λ excitation = 514.5 nm, processed, un-oriented).

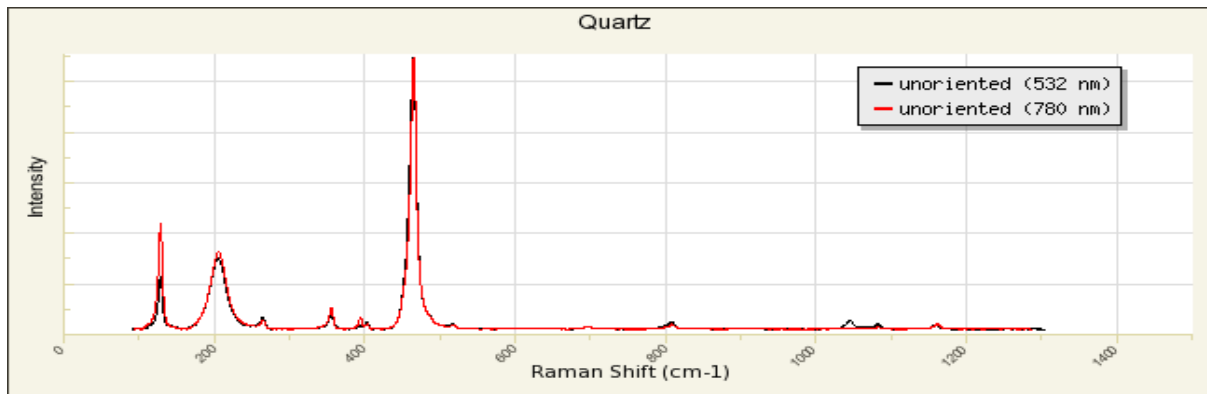


Figure 4.9: Raman spectra of a quartz sample before thermal enhancement (λ excitation = 532 and 780 nm, processed, un-oriented).

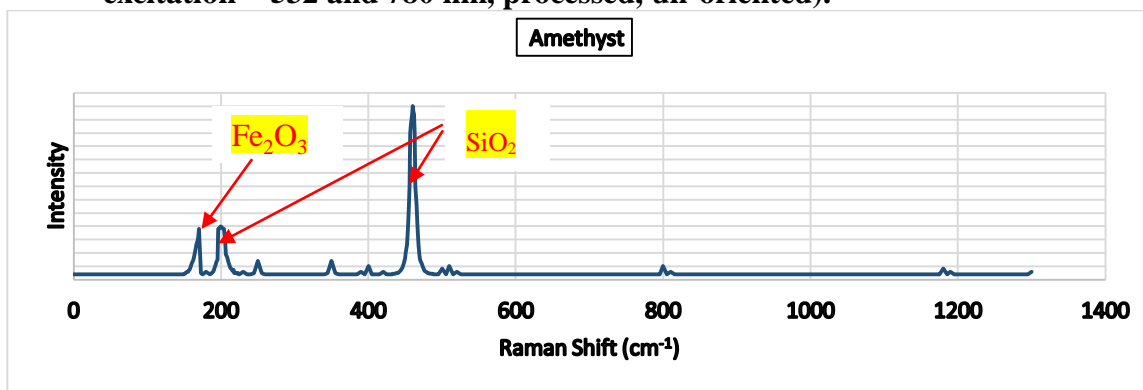


Figure 4.10: Raman spectra of amethyst sample gem after thermal enhancement (λ excitation = 514.5 nm, processed, un-oriented).

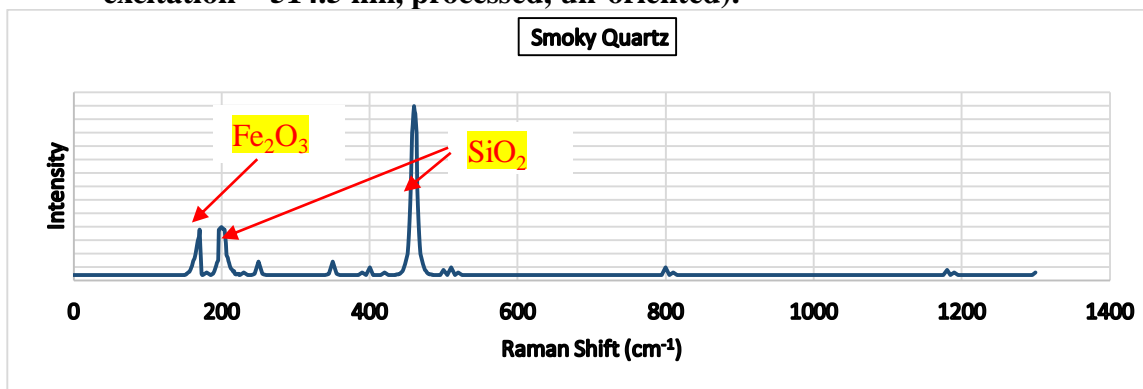


Figure 4.11: Raman spectra of smoky quartz sample after thermal enhancement (λ excitation = 514.5 nm, processed, un-oriented).

The results in Figure 4.6, 4.7, 4.8, 4.9, 4.10 and 4.11 show the Raman spectra for the raw gems and the thermally enhanced gem samples. For the ruby gem (Fig.4.7), the most intense peak was associated with Cr^{3+} luminescence centres at 693 nm ($^{514.5}4366 \text{ cm}^{-1}$) and 694 nm ($^{514.5}4396 \text{ cm}^{-1}$) positions (the suffix 514.5 is the wavelength of the laser used for excitation of the sample). The

Raman peaks which should be located in area shown in Fig. 4.7, were overwhelmed by the luminescence peaks in this spectrum and therefore not evident in this study.

For the blue sapphire gem (Fig. 4.8), seven raman peaks in the position of 378cm^{-1} , 416cm^{-1} , 432cm^{-1} , 578cm^{-1} , 645cm^{-1} , 451cm^{-1} and 751cm^{-1} were observed. The raman Spectra shows peaks characteristic to Al_2O_3 with the most intense peak in the position of 416cm^{-1} and 378cm^{-1} while the rest are in the 432cm^{-1} , 578cm^{-1} , 451cm^{-1} , 751cm^{-1} and 645cm^{-1} positions. Due to the presence of Fe^{3+} a peak at 410cm^{-1} position was observed, which shows the presence of haematite Fe_2O_3 . In relation to the high amount of Al_2O_3 in comparison to Fe_2O_3 no other haematite peak is observed.

For the amethyst and smoky quartz samples (Fig. 4.10 and Fig. 4.11), there were three major Raman peaks observed. Two of the peaks were associated with SiO_2 presence at 205 cm^{-1} and 463 cm^{-1} , and the other one the presence of Fe_2O_3 at 295cm^{-1} . In reference to the Raman mode analysis, there is a predicted that 13 active Raman modes of quartz existed at room temperature conditions (Jasinevicius, 2009), but as the sample is heated, some of the peaks decrease in frequency and utterly disappear. The most intense SiO_2 peak, is caused by Si-O-Si bending and is centered at 463 cm^{-1} while the second most intense peak, associated with a soft mode, is centered at 205 cm^{-1} . Due to the presence of Fe^{3+} we notice an intense peak at 295cm^{-1} position which shows the presence of haematite Fe_2O_3 . There was no evidence of the presence of Al^{3+} peaks in the smoky quartz sample in this study.

4.3.3 The morphological effects of the thermal enhancement on the gems samples

Fig. 4.12 shows the positions of Al_2O_3 diffraction peaks for the corundum samples. It's important to note that sapphire and ruby have an identical crystal structure since Al and O are arranged the same in a trigonal structure. The interatomic distances(d) determines the diffraction peaks which in this study are along the miller indices of 012, 104, 110, 006, 113, 202, 024, 116 and 211 in the 2θ positions of 25.5° , 35° , 38° , 43.5° , 52.5° , 57.5° , 61.5° , 66.5° , and 68° respectively. Heating below the melting point of corundum ensured the crystal structure remained the same and no amorphous structure or change in the crystal structure was observed.

For the quartz samples (Fig. 4.13), shows the positions of SiO_2 diffraction peaks. This is α phase quartz sample crystal structure. The two most significant peaks of α phase quartz determined by the interatomic distance (d) are in the 110 and 101 miller indices in the 2θ positions of 21° and

27° respectively.

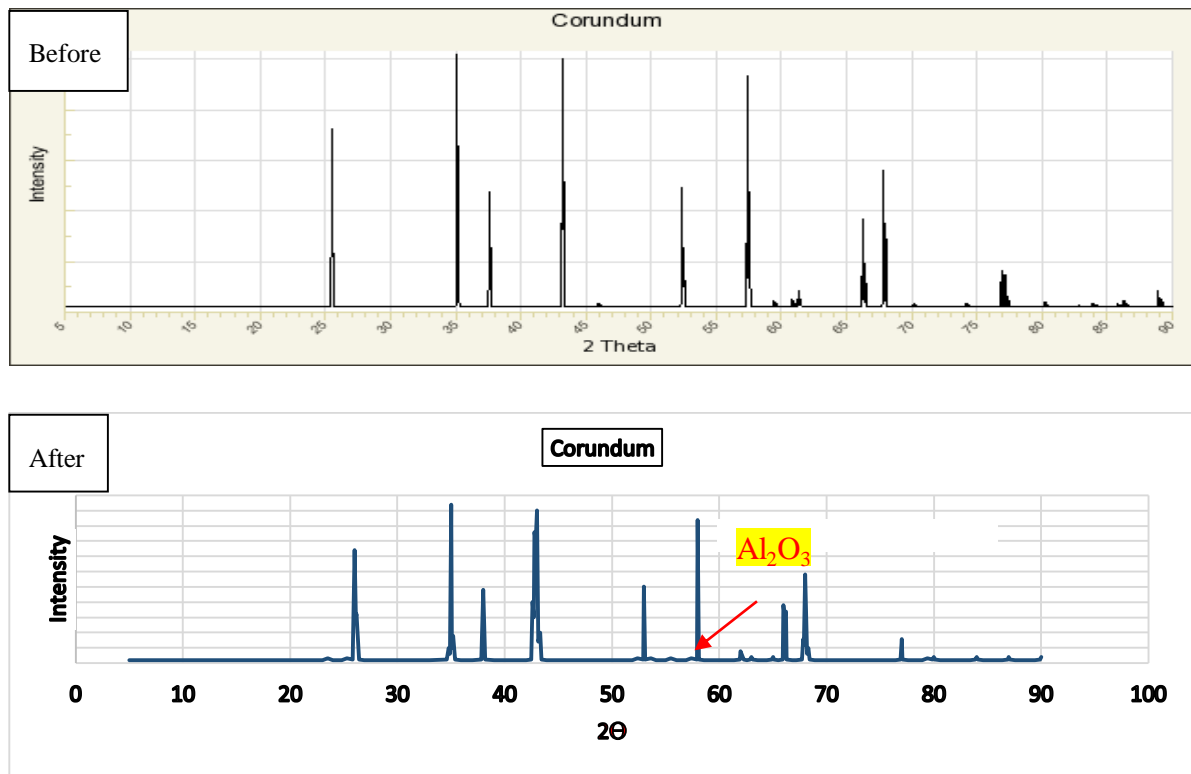
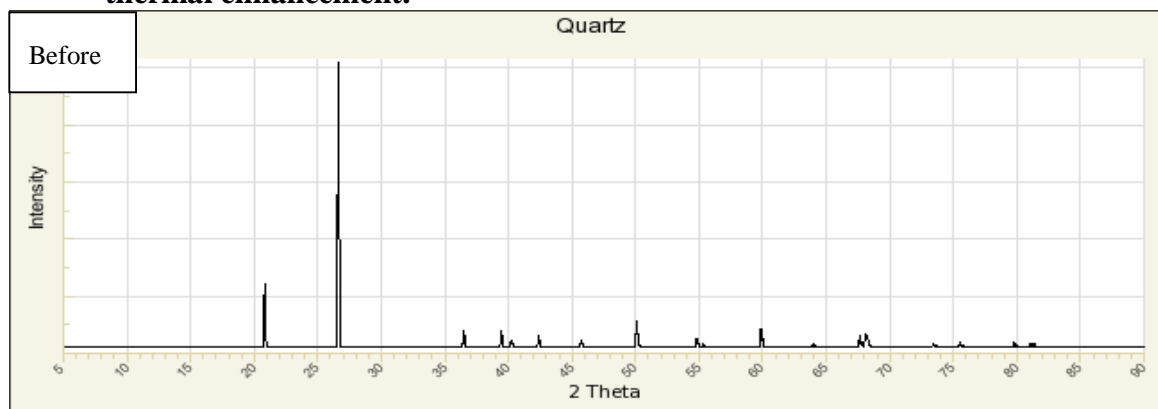


Figure 4.12: X-Ray Diffraction spectra of corundum sample before and after thermal enhancement.



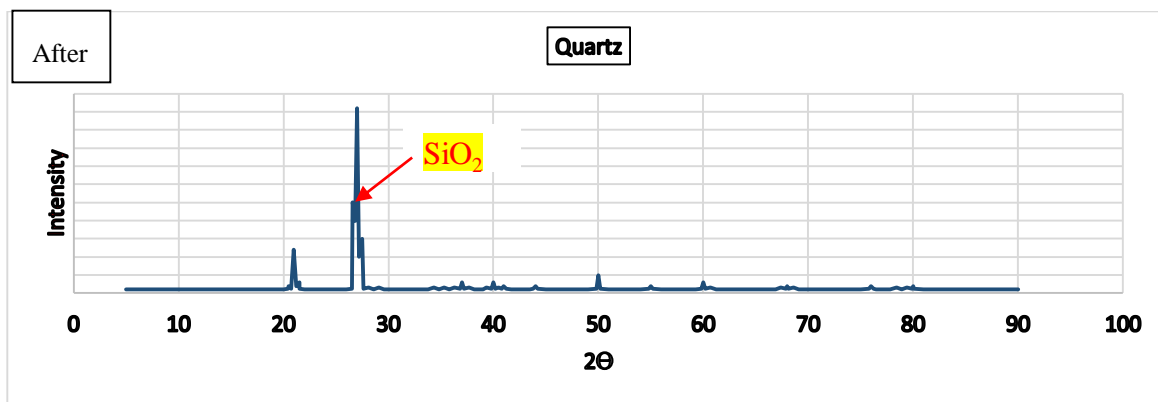


Figure 4.13: X-Ray Diffraction spectra of quartz sample before and after thermal enhancement.

4.4 Comparison of thermally enhanced gems from various parts of the Mozambique belt

Table 4.7 below outlines the differences between thermally enhanced gem samples from Taita-Taveta, Kenya and those enhanced samples from other countries that lie along the Mozambique belt.

Table 4.7: Similarities and Differences between thermally enhanced gem samples from Taita-Taveta in Kenya and enhanced gems of the Mozambique belt.

Gems from Taita-Taveta Region in Kenya	Gems from other Areas in the Mozambique belt
RUBIES	
Physical properties	
Color turned from pink to rose pink to red then deep red. Clarity was enhanced. Development of a silky luster and removal of the purplish hue	Color turned pink to red to deep red. Clarity was very enhanced in most cases. Development and removal of a silky luster and removal of purplish hue (Nassau, 1996 Rankin, 2002; Pardieu, 2010b).
Mineralogical , Chemical and Morphological Properties	
Chemical composition- Al_2O_3 where Al^{3+} is replaced by Cr^{3+} .	Chemical composition - Al_2O_3 where Al^{3+} is replaced by Cr^{3+} , trace amounts of V^{3+} and

<p>Raman Spectroscopy: Cr³⁺ Luminescence observed with no Raman peaks.</p> <p>Crystal structure: Trigonal system of Al₂O₃ with 9 XRD scattering peaks.</p>	<p>Fe³⁺ (Smith et al., 1997; Fritsch and Rossman, 1988a).</p> <p>Raman Spectroscopy: Cr³⁺ Luminescence observed with no Raman peaks (Gaft et al., 2005).</p> <p>Crystal structure: Trigonal system of Al₂O₃ with 9 XRD scattering peaks.</p>
SAPPHIRES	
Physical properties	
<p>Color turned from blue to light blue to white to blue to a deeper blue. Clarity was enhanced. Development of a silky luster and removal of the purplish hue.</p>	<p>Color (blue) was lighted, darkened or developed. Clarity was enhanced. Development or removal of silky luster, reduction of color zoning and reduction of blue patches (Kyi et al., 1999; Rankin, 2002 Maxwell, 2002).</p>
Mineralogical , Chemical and Morphological Properties	
<p>Chemical composition-Al₂O₃ Where Al³⁺ is substituted by Fe²⁺ and Ti⁴⁺</p> <p>Raman Spectroscopy: Al₂O₃ and Fe₂O₃ Raman peaks observed with 7 active modes observed.</p> <p>Crystal structure: Trigonal system of Al₂O₃ (Al-O octahedral sites) with 9 XRD scattering peaks.</p>	<p>Chemical composition- Al₂O₃ Where Al³⁺ is substituted by Fe²⁺ and Ti⁴⁺ and in some cases Ga (Maxwell, 2002)</p> <p>Raman Spectroscopy: Al₂O₃, Fe₂O₃, and TiO₂ Raman peaks observed and in some instances SiO₂ and ZrO₂ peaks caused by Photoluminescence of zircon impurities depending on sample. e.g. Zircon inclusion are considered a distinctive feature for the Madagascar (Ilakaka), Tunduru in Tanzania and Sri Lanka sapphires (Schwarz, 1996; Rankin, 2003; Wang et al., 2006a; Chitty, 2009)</p> <p>Crystal structure: Trigonal system of Al₂O₃</p>

	(Al-O octahedral sites) with 9 XRD scattering peaks.
AMETHYST	
Physical properties	
Color turned from purple to black to dark grey to clear to light yellow to yellow.	Color turned purple to yellow or purple to colorless (Nassau, 1996)
Mineralogical , Chemical and Morphological Properties	
Chemical composition- SiO ₂ where Si ⁴⁺ is replaced by Fe ³⁺ and Fe ²⁺ with minor traces of Ti ⁴⁺ . Raman Spectroscopy: SiO ₂ Raman peaks observed, 2 major Raman peaks. (Sato and McMillan, 1987) and one major peak of Fe ₂ O ₃ Crystal structure: Trigonal system of α phase SiO ₂ (Si-O-Si tetrahedral sites)	Chemical composition- SiO ₂ where Si ⁴⁺ is replaced by Fe ³⁺ and Fe ²⁺ with minor traces of Ti ⁴⁺ . Raman Spectroscopy: SiO ₂ Raman peaks observed, 2 major Raman peaks. (Sato and McMillan, 1987) or in some cases at 573°C of heating, one of the major Raman scattering peaks disappears. (Jenkins and Larsen, 2004). Peaks of Fe ₂ O ₃ , Fe ₃ O ₄ , TiO ₂ and FeTiO ₃ may also be observed. Crystal structure: Trigonal system of α phase SiO ₂ (Si-O-Si tetrahedral sites) or hexagonal system of β phase SiO ₂ (Jasinevicius, 2009).
SMOKY QUARTZ	
Physical Properties	
Color turned from grey to black to rose pink grey to grey to clear to yellow to deeper yellow(golden brown).	Color turned from grey to pale brown, grey to blue green, pink to light pink, and pink to colorless. (Maschmeyer et al., 1980; Goreva et al., 2001)
Mineralogical , Chemical and Morphological Properties	
Chemical composition- SiO ₂ where Si ⁴⁺ is replaced by Al ³⁺ and small alkali ions of Li ⁺ and Na ⁺ with traces of Fe ³⁺ . Raman Spectroscopy: SiO ₂ Raman peaks	Chemical composition- SiO ₂ where Si ⁴⁺ is replaced by Al ³⁺ and small alkali ions of Li ⁺ and Na ⁺ with traces of Fe ³⁺ . Raman Spectroscopy: SiO ₂ Raman peaks

<p>observed with 2 major Raman peaks and one major peak of Fe₂O₃</p> <p>Crystal structure: Trigonal system of α phase SiO₂ (Si-O-Si tetrahedral sites) with 2 major XRD scattering peaks.</p>	<p>observed, 2 major Raman peaks. (Sato and McMillan, 1987) or in some cases at 573°C of heating, one of the major Raman scattering peaks disappears (Jenkins and Larsen, 2004). Peaks of Al₂O₃ are also observed</p> <p>Crystal structure: Trigonal system of α phase SiO₂ (Si-O-Si tetrahedral sites) or hexagonal system of β phase SiO₂ (Jasinevicius, 2009).</p>
--	--

The similarities in the physical, mineralogical, chemical and morphological properties of the gems after thermal enhancement (Table 4.7), are due to the fact that the gems from the Mozambique belt including Taita-Taveta, share similar geochemistry due to the same geological formation (See appendix A). In addition, it is also due to common thermal enhancement procedures used for each gem depending on the purpose of the procedure.

For the quartz samples (amethyst and smoky quartz), the temperatures used are similar to the ones used by other researchers, resulting in similar optimization temperatures i.e. in this research, amethyst turned to Citrine between 450°C -550°C while in Sri Lanka, amethyst turned to citrine at temperatures between 470°C - 770°C (Nassau, 1996).

The differences in color and other physical properties (Table 4.7), may be accounted to the difference in the thermal enhancement procedures. The procedures depend on the purpose of the thermal enhancement process either to lighten the color, darken the color, reduce the color zoning, reduce the color patches, create a new color, remove or develop silk. The thermal enhancement procedure is dependent on the (1) Maximum temperatures attained. (2) How long the maximum temperature is sustained. (3) Rate of heating to the maximum temperatures. (4) Rate of cooling down from the maximum temperatures and any holding stages while cooling. (5) The pressure of the atmosphere. (6) Chemical nature of the atmosphere. (7) The nature of material contact in furnace with gemstone. (8) Quality of gemstone used (9) Different temperatures used for different periods of time. (10) Cooling conditions. The colors and other physical properties therefore

produced are dependent on which procedure is used to get the best desired effects, and this is subject to the researcher.

In this research the maximum temperatures reached were 1200°C, heated at a temperature gradient of 50°C in an oxidizing environment and the time of heating was 3-6 h depending on the gem sample. For the Corundum samples (rubies and sapphires), low temperatures were used compared to the temperatures used for corundum sample enhancement in other researches (1300°C, 1400°C, 1500°C and 1600°C) (Nassau, 1996; Hughes, 1997, Pardieu, 2010b). This could be the reason why the results are different despite the shared geochemistry.

The differences observed in Raman Spectroscopy were because of the sensitivity of instrument used where the amounts of different ions in the gem may be too little for the peaks to be noticed. In reference to the Raman mode analysis, there is the predicted 13 active Raman modes in quartz at room temperature, but as the sample is heated, some of the peaks decrease in frequency and may utterly disappear (Jasinevicius, 2009). In some cases, the particular gem sampled may contain an increased or decreased amount of some chemical ions than another sample in the same area. For example, Pardieu (2010b) records a corundum sample from Niassa area in Mozambique to contain Cr, Ti, Fe, V and Ga using EDXRF as the method of analysis.

Crystal orientation caused some peaks to be evident or lacking in the case of Raman Spectroscopy. As for minerals with uniaxial indicatrices the Raman peak intensity changes with change in the laser polarization. The uniaxial optical indicatrix (trigonal and hexagonal), has a circular cross-section meaning it's only in one orientation (Jasinevicius, 2009), like in the case of all the gems selected for this study e.g., corundum. Porto and Krishnan (1967) and Xu et al. (1995) observed that the Raman peaks at 576, 643, and 749 cm^{-1} in corundum disappear, when polarization of the incident beam is parallel to the c-axis. However, when it is oriented with the incident laser beam parallel to the a-axis, the cross-section changes to an ellipse, therefore altering the peaks intensities greatly with rotation. This is due to the change of the atomic vibrations degree of freedom. In the first instance when the indicatrix is circular, there is no significant change in peak intensities since the atomic vibrations are equally distributed in all directions (Jasinevicius, 2009). In spite of the above conclusions about the orientation dependence on the Raman peaks of corundum, the peaks can be precisely identified using a spectrum of a randomly oriented sample like in the case of this

study.

Differences were also due to how some ions react under Raman Spectroscopy. Some of the corundum gems may also contain REE which may cause fluorescence features that may overwhelm the Raman spectra. The REE may also cause metamictization which is loss of crystallinity. Metamictization has dramatic effects on the Raman spectra which include decrease in peak intensities, disappearance of peaks, shifts in peak frequencies and increase of peak widths e.g. in the Sri Lanka and Madagascar (Ilakaka) Sapphires with significant zircon inclusions where Hf^{4+} ions replace Zr^{4+} up to 6 Hf: 10Zr and other REE as U and Th commonly replace some of the Zr or in the case of heating a quartz sample at 573°C , one of the major Raman scattering peaks disappears (Phillips and Griffen, 2004).

The deviations in X-Ray diffraction peaks were due to the differences in the crystal structure as in the case of heating a quartz sample at more than 573°C . In some cases, this changes the trigonal system of the α phase quartz (Si-O-Si tetrahedral sites) to a hexagonal system of β phase quartz (Phillips and Griffen, 2004). Since the Si and O atoms are arranged differently for the α phase quartz and the β phase quartz, there are two different X-Ray Diffraction scattering patterns observed. In this study the researcher observed the α phase quartz even after heating.

CHAPTER 5

CONCLUSIONS AND RECOMMENDATIONS

5.1 Conclusions

This study determined the physical, mineralogical, chemical, and morphological effects of an optimized thermal enhancement process on gemstones using X-Ray Diffraction and Raman Spectroscopy.

The first objective was to analyze how thermal enhancement affects the color of the gems. The gems were heated in a controlled environment in a Muffle furnace with a maximum temperature of 1200°C. The duration of the heat treatment was between a few minutes to several hours depending on the type of gemstone, the color desired, and the necessary temperatures required to achieve the desired color. The study established that the color changed for each gem sample selected as the temperature increased.

The second objective was to optimize the thermal enhancement process for the specific gem samples. The temperature was recorded every time the color changed for each sample gem until the desired physical properties were achieved. The study established that each gem sample changed color several times with an increase in temperature till an optimum temperature was reached. The optimum temperature was where an expected change in color, enhanced clarity, the deepness of color, permanence of color, and reduction in zoning occurred. The optimum temperature for rubies and sapphires was 12000C, 4500C -5500C for amethyst, and 6000C -6500C for smoky quartz.

The third objective was to determine the thermal enhancement process's physical, mineralogical, chemical, and morphological effects on the gems samples. Physical changes of the heated gem samples were recorded and compared to untreated raw samples. The mineralogical, chemical, and morphological effects of thermally enhanced gem samples, were analyzed using Raman Spectroscopy and XRD powder method and compared with the existing data on the RRUFF mineral database. The study established physical and chemical changes of gems after enhancement. However, there were no morphological changes observed.

The last objective was to compare the physical, mineralogical, chemical, and morphological effects of thermally enhanced gems from Taita-Taveta to those from other areas in the Mozambique belt. This study compared the results from sub-sections 4.1, 4.2, and 4.3 above with other documented effects from similar samples in the Mozambique belt. It was established that there were similarities and differences between the physical, mineralogical, chemical, and morphological properties of the gems of Taita-Taveta and those from other areas of the Mozambique belt. The similarities are due to gems' shared geology and geochemistry in the Mozambique belt. They were also due to the thermal enhancement procedures used for each gem depending on the purpose of the procedure. The deviations were accounted to the difference in the thermal enhancement procedures used, which depend on the purpose of the thermal enhancement process to lighten or darken the color, reduce the color zoning, reduce the color patches, create a new color, remove or develop silk. The difference would also have been due to the instrument's sensitivity. For instance, the muffle furnace in this study reached maximum temperatures of 1200oC. In the Raman Spectroscopy, the differences could have been due to the amounts of different ions in the gem being too little for peaks to be noticed or overwhelmed by the REE photoluminescence peaks.

Given these findings, the ruby, sapphire, amethyst, and smoky quartz samples' quality was significantly improved from grade D gems to Grade C and from Grade C to Grade B (See appendix E). This means that changes in the gems' physical appearance, mineralogy, and chemistry caused an improvement in color, clarity, and luster, hence improving the overall gem quality.

5.2 Recommendations

The thermal enhancement process can improve gem-quality by changing their mineralogy, chemistry, and morphology, i.e., color, clarity, and luster. This enhancement process is relatively cheap and can be used for varied gems other than those outlined in this study.

The thermal procedures used in this research showed that the stability of colors is semi-permanent. When exposed to sunlight, the gemstones take a few days to return to their original colors. Further research should be carried out on how to stabilize the enhanced color.

Optimization procedures for the thermal enhancement processes for gems are outlined to increase accuracy, hence minimizing losses (financial or otherwise) of trial and error methods used by small-scale miners from the area. The information in this study would help a researcher understand

the cause of color in a particular gem and how heating affects the ions involved and would therefore help draft a procedure with the expected results in mind.

The mineralogical, chemical, and morphological effects of the thermal enhancement process of the gems can be quantified using X-Ray Diffraction powder and Raman Spectroscopy methods of analysis. This analysis method can also be used to test if other gems in the market have undergone enhancement.

Further research should be carried out to outline more optimization procedures for the gems in Kenya, using muffle furnaces of higher maximum temperatures than 1200OC. Other enhancement processes, in addition to the thermal enhancement, can be used to improve the low-grade gems and thus their value in the international gem market.

REFERENCES

- Abduriyim A., Kitawaki, H. (2006). Applications of laser ablation-inductively coupled plasma-mass spectrometry (LA-ICP-MS) to gemology. *Gems and Gemology*, 42, 98 - 118.
- Andriessen P.A.M., Coolen J.M., Hebeda, E.H. (1985). K-Ar hornblende dating of late PanAfrican metamorphism in the Furua granulite complex of southern Tanzania. *Prec. Research*, 30, 351-360.
- Ashbaugh C.E. (1988). Gemstone irradiation and radioactivity. *Gemstones and Geology*, 24(4), 196-213.
- Ashbaugh C.E. (1992). Gamma Ray Spectroscopy to measure radioactivity in Gemstones. *Gems and Gemology*, 28(2), 104-111.
- Bancroft P. (1984). Gem and Crystal Treasures, Western Enterprises Mineralogical Record, Fallbrook, CA, 488 (also published in Palagems.com).
- Bideaux R.A., Blath K. W., Nichols M. C., (2003). Handbook of Mineralogy. Mineral Data Publishers, Tucson. AZ, 5, 45 -216.
- CalTech (California Institute of Technology) (2009). Vibrational Raman Spectroscopy, Dynamical Light Scattering and Resonance Raman Spectroscopy of Cytochrome. BILRC Laser lab GLA, 2.
- Cahen L., Snelling, N.J. Delhal, T. and Vail J.R. (1984). The Geochronology and Evolution of Africa. Oxford, Clarendon Press, 512.
- Carey P.R. (1982). Biochemical Applications of Raman and Resonance Raman Spectroscopies, Academic Press.
- Cesbron F., Lebrun P., Le Cléac. 'H, J.M., Notari F., Grobon C., Deville, J. (2002). Corindons et spinelles. *Minéraux et Fossiles* 15, Paris, France.
- Chalain J.-P. (1995). Observations and identification of treated fissures in rubies. *Antwerp Facets Annual Belgian Diamond Report* 95, 42-43.
- Channel K. (2012). Comparison of the mineralogy and morphology of travertine from the U.S.A and New Zealand.
- Chitty W.G.G. (2009). A study on sapphires and rubies from Tanzania's Tunduru, District. M.sc Thesis.1,12,15 -47.

- Cutten H.N.C. (2002). The Mozambique Belt, Eastern Africa tectonic evolution of the Mozambique Ocean and Gondwana amalgamation. Precambrian Geology, Denver Annual Meeting, Session No 122. Ali, East African Gems Personal communications 2007-2010.
- Cutten M.P. H.N.C, Muhongo B., Waele D. (2003). Neoproterozoic magmatism and metamorphism of the western granulites in the central domain of the Mozambique belt, Tanzania: *Tectonophysics* 375, 25– 145.
- David C., Fritsch E. (2001). Identification du traitement thermique à haute température des corindons par spectrométrie infra-rouge. *Rev. de Gem.*, 141/142, 27–31.
- Dharmaratne P.G.R., Premasiri H.M.R., Dillimuni D. (2012). Sapphires from Thammannawa, Katagarama area, Sri Lanka. *Gems and Gemology*, 48, 98–107.
- Dirlam D., Misiorowski E.B, Tozer R., Stark K.B, Bassett A.M. (1992). Gem wealth of Tanzania. *Gems and Gemology*, 28(2), 80-102.
- Dissanayake C.B. and Chandrajith R. (1999). Sri Lanka – Madagascar Gondwana Linkage; Evidence for a Pan African mineral belt.
- DuBois C., Walsh J. (1970). Minerals of Kenya. Geological Survey of Kenya Bulletin 11.
- Duplessis Y. (1985). *Les Couleurs Visibles et Non Visibles*. Editions du Rocher, Paris.
- Emmett J.L. (1999). Fluxes and the heat treatment of ruby and sapphire. *Gems and Gemology*, Vol. 35(3), 90–92.
- Emmett J.L., Scarratt K., McClure S.F., Moses T.M., Douthit T.R., Hughes R., Novak S., Shigley J. E., Wang W., Bordelon O., Kane R. E. (2003). Beryllium diffusion of ruby and sapphire. *Gems and Gemology*, 39 (2), 84–135.
- Feneyrol J., Giuliani G., Ohnenstetter D., Le Goff E., Simonet C., Rakotondrazafy A.F.M., Ichang'i D., Malisa E., Deschamps Y., Fallick A.E., Khan T. & Nyamai C. (2013). Les gemmes néoproterozoïques de la ceinture métamorphique mozambicaine du supercontinent Gondwana (1000–542 Ma). *le Règne Minéral*, 2,13–50.
- Fritsch E., Rossman G. R. (1987). An Update on Color in Gems, Part 1: Introduction and Colors Caused by Dispersed Metal Ions", *Gems and Gemology*, 23(3),126-139.
- Fritsch E., Rossman G. R. (1988 a). An Update on Color in Gems, Part 2: Colors Involving Multiple Atoms and Color Centers", *Gems and Gemology*, 24 (1), 3- 15.
- Fritsch E., Rossman G. R. (1988 b). An Update on Color in Gems, Part 3: Colors Caused by

- Band Gaps and Physical Phenomena", *Gems and Gemology*, 24 (2), 81 -102
- Gaft M., Reisfeld R., Panczer G. (2005). *Modern Luminescence Spectroscopy of Minerals and Materials*, Springer, Heidelberg, Germany.
- Garnier V., Giuliani G., Ohnenstetter D. & Schwarz D. (2004). Saphirs et rubis. Classification des gisements de corindon. *le Règne Minéral*, 55, 4 - 47.
- Giovanna L. C., Fernando S. L. (2015). Color change of gemstones by exposure to gamma rays. 2015 international nuclear atlantic conference - inac 2015 São paulo, sp, brazil, october 4-9, 2015. Associação brasileira de energia nuclear – aben.
- Giuliani G., Fallick A.E., Rakotondrazafy A.F.M., Ohnenstetter D., Andriamamonjy A., Rakotosamizanany S., Ralantoarison Th., Razanatseheny M.M., Dunaigre C., Schwarz D. (2007). Oxygen isotope systematics of gem corundum deposits in Madagascar: relevance for their geological origin. *Mineral. Deposita*, 42, 251–270.
- Giuliani G., Ohnenstetter D., Fallick A.E., Feneyrol J. (2011). State of the art in the formation of high-value colored gemstones. *Gems and Gemology*, 47, 108–110.
- Giuliani G., Groat L.A. (2012). La géologie des gemmes. *Pour la Science*, 418, 58–65.
- Giuliani G., Groat L., Ohnenstetter D., Fallick A. E., Feneyrol J. (2014a). The Geology of Gems and their geographic origin. *Mineralogical Association of Canada Short Course 44*, Tucson AZ, 113–134.
- Giuliani G., Groat L., Ohnenstetter D., Fallick A.E., Fagan A. J. (2014b). The Geology and Genesis of Gem Corundum Deposits. *Mineralogical Association of Canada Short Course 44*, Tucson AZ, 29-112
- Goreva J.S., Ma, C., Rossman G.R. (2001). Fibrous nano-inclusions in massive rose quartz: The origin of rose coloration. *American Mineralogist*, 86 (4), 466-472.
- Graham I.T., Cook, N.J. (2008). The genesis of gem deposits. *Ore Geol*, 34, 215.
- Groat L.E. (2007). Geology of gem deposits. *Mineralogical Association of Canada, Short Course Series 37*, Yellowknife, Canada, 276.
- Groat L.A. (2012). Gemstones. *Amer. Scientist* 100, 128–137.
- Hall M., Moses T.M. (2000). Blue and pink treated diamonds. *Mazal U'Bracha*, 15 (126), 42–43.
- Harris D. C., Bertolucci M. D. (1990). *Symmetry and Spectroscopy: An Introduction to Vibrational and Electronic Spectroscopy*, Dover Publications.

- Herzberg G. (1991). *Molecular Spectra and Molecular Structure II: Infrared and Raman Spectra of Polyatomic Molecules*, Krieger Publishing.
- Hlava P.F. (1990). *Causes of color in minerals and gemstones*. Sandia National Laboratories Department 1822 Mail Stop 0886 Albuquerque, NM 87185-0886.
- Hughes R.W. (1997). *Ruby and Sapphire*. RWH Publishing, Boulder.
- Hughes R.W., Galibert O. (1998). Foreign affairs: Fracture healing/filling of Möng Hsu ruby. *AusG*, 20 (2), 70–74.
- Hurai V., Wierzbicka M. (2013). X-ray diffraction and vibrational spectroscopy characteristics of hydroxylclinohumite from ruby bearing marbles Luc Yen District, Vietnam
- Jasinevicius R. (2009). characterization of vibrational and electronic features in the raman spectra of gem minerals
- Jenkins A. L., Larsen R. A. (2004). *Gemstone identification using Raman Spectroscopy*
- Johnson M.L., McClure S.F. (2000). GTLN: An investigation of fracture fillers in Mong Hsu rubies. *Gems and Gemology*, 36 (3), 257–259.
- Jöns N. & Schenk V. (2008). Relics of the Mozambique Ocean in the central East African Orogen: evidence from the Vohibory Block of Southern Madagascar. *J. Metam. Geol.*, 26,17–28.
- Kammerling R.C., Koivula J.I., Kane R.E. (1990). Gemstone enhancement and its detection in the 1980s. *Gems and Gemology*, 26, 1, 32–49.
- Kane R. (2008). American sapphires: Montana and Yogo. *World of Gems Conference Proceedings*, September 13–14, 2008, Chicago, Illinois, 9–64
- Keller P.C. (1992). *Gemstones of East Africa*. Phoenix. Geoscience Press, 144.
- Kenya Engineer (2010). *Journal of the Institution of Engineers Intercontinental Publishers Ltd.*, Nairobi, 31, 4.
- Key R., Rop P. (1987). *Geology of the Maralal area*. Geological Survey of Kenya Report 105.
- Key R.L., Hill P.G. (1989). Further evidence for the control on the growth of vanadian grossular garnets in Kenya. *Journal of Gemmology*, 1989, 21, 7.
- Kievlenko E.Y. (2003). *Geology of Gems*. Ocean Pictures Ltd, Littleton, CO, USA.
- Kroner A. (1984). Late Precambrian plate tectonics and orogeny: a need to redefine the term Pan-African. In Klerkx, J. & Michot, J. (Eds), *African Geology*. Tervuren, Musée

- Royal de l'Afrique Centrale, Belgique, 23–28.
- Kroner A. (1991). African linkage of Precambrian Sri Lanka. *Geologische Rundschau*, 80 (2), 429-440.
- Krzemnicki M.S. (2010). How to get the blues out of the pink: Detection of low-temperature treatment of pink sapphires? Presentation to Hong Kong Jewellery Show, March.
- Kyi H., Buchholz P., Wolf D. (1999). Heat treatment of milky sapphires from the Mogok stone tract, Myanmar. *Journal of Geodynamics*, 26(5), 313–315.
- Laserna J. J. (2006). An Introduction to Raman Spectroscopy: Introduction and Basic Principles. <http://www.obs.univbpcclermont.fr/sfmc/ramandb2/index.html>
- Le Goff E., Deschamps Y., Guerrot C. (2010). Tectonic implications of new single zircon Pb–Pb evaporation data in the Lossogonoi and Longido ruby-districts, Mozambican metamorphic Belt of north-eastern Tanzania. *C. R. Geoscience*, 342, 36–45.
- Lexi M.N. (2002). Grading of gemstones. *Customer Advocate, Research and Resource Development Group, Exclusively for Fire Mountain Gems and Beads*, 12(3), 34-35
- Long D. A. (2002). The Raman effect. A unified treatment of the theory of Raman scattering of molecules. *Wiley Chichester*, 21, 12-67.
- Malisa E. & Muhongo S. (1990). Tectonic setting of gemstone mineralization in the Proterozoic metamorphic terrane of the Mozambique Belt of Tanzania. *Precambrian Research*, 46, 167-176.
- Maschmeyer D., Niemann K., Hake H., Lehmann G. & Räuber A. (1980). Two modified smoky quartz centers in natural citrine. *Physics and Chemistry of Minerals*, 6(2), 145-156.
- Maxwell M. (2002). The processing and heat treatment of Subera (Queensland) sapphire rough. *AusG*, 21(8), 279–286.
- McClure S. F. & Smith C. P. (2000). Gemstone Enhancement and Detection in the 1990s. Enhancement in the 1990s, *Gems and Gemology*, Winter 2000, 36(4), 336–359
- McClure S. F., Kane R. E., Sturman N. (2010). Gemstone Enhancement and Detection in the 2000s. *Gems and Gemology*, 46(3), 218–240.
- Mercier A., Debat P., Saul J.M. (1999a). Exotic origin of the ruby deposits of the Mangari area in SE Kenya. *Ore Geol. Rev.* 14, 83–104.
- Mercier A., Rakotondrazafy A.F.M. & Ravolomiandrinarivo B. (1999b). Ruby mineralization

- in Southwest Madagascar. *Gondwana Res.* 2, 233–238.
- Mghanga M. (2011). *Mining in Taita-Taveta, Prospects and Problems*, Heinrich Böll Foundation East and horn of Africa, Nairobi. Think Interactive Limited, 15 - 44
- Mosley P. (1993). Geological evolution of the late Proterozoic " Mozambique Belt " of Kenya. *Tectonophysics*, 221, 223-250.
- Muhlmeister S., Fritsch E., Shigley J.E., Devouard B., Laurs B.M. (1998). Separating natural and synthetic rubies on the basis of trace element chemistry. *Gems and Gemology*, 34, 80 - 101.
- Muhongo S. (1998). Anatomy of the Mozambique belt of eastern and southern Africa. *Journal. Afr. Earth Sci.*, 27, 142.
- Narendra N. G., Amit B. R. (2011). *Handbook of Benzoxazine Resins*.
- Nassau K. (1980). The Causes of Color", *Scientific American*, 243(4), 124 – 154.
- Nassau K. (1983). *The Physics and Chemistry of Color: The Fifteen Causes of Color*, John Wiley & Sons, New York, 454, 3.
- Nassau K. (1984). *Gemstone Enhancement*. Butterworth-Heinemann Ltd, Oxford. 114- 271
- Nassau K. (1985). Altering the color of topaz. *Gems and Gemmology*, 21(1), 26–34,
<http://dx.doi.org/10.5741/GEMS.21.1.26>
- Nassau K., Valente G. K. (1987). The Seven Types of Yellow Sapphire and Their Stability to Light", *Gems and Gemology*, 23(4), 222 – 231
- Nassau K. (1996). *Gemstone Enhancement*. Butterworth Heinemann, Oxford. 21- 168
- Nyamai C.M., Mathu E.M., Akech N. O. and Wallbrecher E. (2003). A Reappraisal of the Geology, Geochemistry, Structures and Tectonics of the Mozambique belt in Kenya, East of the Rift System. *African Journal of Science and Technology (AJST) Science and Engineering Series* 4(2), 51-71.
- O'Donoghue M. (2006). *Gems*, Elsevier, Oxford, UK.6, 221-314.
- Olivier B. (2006). *Geology and Petrology of the Merelani Tanzanite Deposit, NE Tanzania*, PHD Thesis University of Stellenbosch, South Africa Pallister, The Tectonics of East Africa. *Tectonic of Africa*, United Nations Educational, Scientific and Cultural Organization., Paris, 6, 511-543.

- Oso W. Y., Onen D. (2009). A general guide to writing research proposal and report. 1, 120-145.
- Paradise T.R. (1982). The natural formation and occurrence of green quartz. *Gems & Gemology*, 18(1), 39.
- Pardieu V. (2007). Tanzania Oct 2007, a gemological safari. www.fieldgemology.org.
- Pardieu V., Hughes R.W., Soubiraa M. R., Brunot P., Brunot M. C., Brunot W. (2010a). working the Blueseam: The Tanzanite Mines of Merelani; <http://www.ruby-sapphire.com/tanzania-tanzanite-mines.html>
- Pardieu V., Sturman N., Saeseaw S., DuToit G., Thirangoon K. (2010b). FAPFH/GFF Treated ruby from Mozambique. www.gia.edu/researchresources/news-from-research/Flux_heated_and_glass_filled_rubies_from_Mozambique_edu.pdf, May 11.
- Peretti A., Schmetzer K., Bernhardt H. J., Mouawad F. (1995). Rubies from Mong Hsu. *G&G*, 31(1), 26.
- Phillips W.R., Griffen D.T. (2004). *Optical Mineralogy*. 3(24),314-323.
- Pohl W., Niedermayr G. (1979). Geology of the Mwatate Quadrangle and the vanadium grossularite deposits of the area. Geological Survey of Kenya Report 101.
- Pohl W., Niedermayr G. (1980). Geology of the Mwatate Quadrangle and the Vanadium Grossularite Deposits of the Area. 101, 55
- Porto S.P.S., Krishnan R.S. (1967). Raman Effect of Corundum. *The Journal of chemical physics*, 47, 1009.
- Rakotondrazafy M., Giuliani G., Fallick A.E., Ohnenstetter D., Andriamamonjy A., Rakotosamizanany S., Ralantoarison Th., Razanatseheno M., Offant Y., Garnier V., Maluski H., Dunaigre Ch., Schwarz D., Mercier A., Ratrimo V. & Ralison B. (2008). Gem corundum deposits in Madagascar: a review. *Ore Geol. Rev.* 34, 134 - 154.
- Rankin A.H. (2002). Natural and heat-treated corundum from Chimwadzulu Hill, Malawi: Genetic significance of zircon clusters and diaspore-bearing inclusions. *Journal of Geodynamics*, 28(2), 65–75.
- Rankin A.H., Edwards W. (2003). Some effects of extreme heat treatment on zircon inclusions in corundum. *Journal of Geodynamics*, 28(5), 257–264.
- Reinitz I.M., Buerki P.R., Shigley J.E., McClure S. F., Moses T.M. (2000). Identification of

- HPHT-treated yellow to green diamonds. *Gems and Gemology*, 36(2), 138–146.
- Rossmann G. R. (1981). Color in Gems: The new technologies. *Gems and Gemology*, 18(2), 87–89.
- Rupasinghe M.S., Dissanayake C.B. (1985). Charnockites and the genesis of gem minerals. *Chem. Geology*, 53, 1–16.
- Salama S.M. S. (2011). Study on Properties of Some Treated Gemstones. PhD Thesis, Benha University, Faculty of Science, Physics Department, RPF, ETRR-2, Atomic Energy Authority.
- Santosh M. and Collins A.S. (2003). Gemstone mineralization in the Palghat-Cauvery shear zone system (Kakur-Kangayam belt), Southern India. *Gondwana Res.* 6, 911 - 918.
- Sato R.K. & McMillan P.F. (1987). An infrared and Raman study of the isotopic species of alpha-quartz. *Journal of Physical Chemistry*, 91(13), 3494–3498.
- Schmetzer K. & Schwarz D. (2007). Color zoning in heat-treated yellow to yellowish-orange Montana sapphires. *Journal of Geodynamics*, 30(5/6), 268–278.
- Schwarz D., Petsch E.J., Kanis J. (1996). Sapphires from the Andranondambo region, Madagascar. *Gems and Gemology*, 32(2), 80–99.
- Schwarz D., Pardieu V., Saul J.M., Schmetzer K., Laurs B.M., Giuliani G., Klemm, L., Malsy A.K., Hauzenberger C., Du Toit G., Fallick A.E. & Ohnenstetter D. (2008). Ruby and sapphires from Winza (central tanzania). *Gems & Gemology*, 44, 322–347.
- Scmid T. & Dariz P. (2019). Raman Spectroscopy. *The Heritage*, 2(2), 1662- 1685
- Shapiro S.M., O'Shea D.C., Cummins H.Z. (1967). Raman scattering study of the alpha-beta phase transition in quartz. *Physical Review Letters*, 19(7), 361–364.
- Shibata K. (1975). Preliminary Geochronological Study on Metamorphic Rocks from the Taita Hills, Southern Kenya. *African Studies*, Nagoya University (Japan); 72—75.
- Shigley J.E., Dirlam D.M., Laurs B.M., Boehm E.W., Bosshart G., Larson W.F. (2000a). Gem localities of the 1990s. *G&G*, 36(4), 292–335.
- Shigley J.E., McClure S.F., Koivula J.I., Moses T.M. (2000b). New filling material for diamonds from Oved Diamond Company: A preliminary study. *Gems and Gemology*, 36(2), 147–153.
- Shigley J.E., Laurs B.M., Janse A.J.A. (Bram), Elen S., Dirlam D.M. (2010). Gem localities of the 2000s. *G&G*, 46(3), 188–216.

- Shor R., Weldon R. (2009). Ruby and sapphire production: A quarter century of change. *Gems and Gemology*, 45(4), 236–259.
- Silva K.K.M.W & Siriwardena C.H.E.R (1988). Geology and the origin of the corundum-bearing skarn at Bakamuna, Sri Lanka. *Mineral. Deposita* 23, 186–190.
- Simonet C. (2000a). Géologie des gisements de saphir et de rubis- L'exemple de la John Saul Ruby Mine, Mangare, Kenya, PhD thesis. University of Nantes.
- Simonet C. (2000b). Geology of the Yellow Mine (TaitaTaveta District, Kenya) and other yellow tourmaline deposits in East Africa. *Journal of Gemology*, 27(1), 1129.
- Simonet C. (2000c). The John Saul Mine (Mangare area, Southern Kenya) - Current activity and production. *Gems and Gemology* in press. 44 - 98
- Simonet C., Okundi S., Masai P. (2001). General setting of colored gemstone deposits in the Mozambique Belt of Kenya—preliminary considerations. *Proc. 9th Conf. Geol. Soc. Kenya*, Nairobi, Nov 2000, 123–138.
- Simonet C., Okundi S., Masai P. (2002). General setting of colored gemstone deposits in the Mozambique belt of Kenya – Preliminary considerations. In Nyamai, C.M. and Maimba, M. (eds.) *Proceedings of the 8th and 9th Regional Conference of the Geology of Kenya*, Pub. Geol. Soc. Kenya, 123-138.
- Simonet C., Fritsch E., Lasnier B. (2008). A classification of gem corundum deposits aimed towards gem exploration. *Ore Geol.* 34, 127–133
- Smith C.P., Gübelin E.J., Bassett A.M., Manandhar M.N. (1997). Rubies and fancy-color sapphires from Nepal. *Gems & Gemology*, 33(1), 24–41.
- Smith C., Quinn D. E., Woodring H. S. (2008a). Inside pink diamonds. *RDR*, 31(11), 1, 49–56.
- Smith C., Quinn D. E., Woodring H. S. (2008b). Inside blue diamonds. *RDR*, 31(35), 1, 48–56.
- Smith C., Beesley C.R., Quinn D. E., Mayerson W.M. (2008c). Inside rubies. *RDR*, 31(47), 140–148.
- Suleman A. (1999). Colored stones in Africa and Madagascar. *Gems and Gemology* 35(3), 66-67.
- TTCDP - Taita Taveta County Development Plan. (2012). The first Taita Taveta county integrated development plan 2013-2017. 23- 78

- Thomas E. (2006). Crystal growth and search for highly correlated ternary intermetallic antimonides and stannides.
- Walsh J. (1960). Geology of the Area South of the Taita Hills. 49 (1957), 26, Geol. Survey Kenya, Nairobi 1960. Geology of the Ikutha Area. 56 (1959), 37, Geol. Survey Kenya, Nairobi 1963.
- Walton L. (2004). Exploration Criteria for Color Gemstone Deposits in the Yukon, Yukon Geological Survey, 184 (Open File 2004-10)
- Wang W., Tallaire A., Hall M.S., Moses T.M., Achard J., Sussmann R.S., Gicquel A. (2005). Experimental CVD synthetic diamonds from LIMHP CNRS, France. *Gems and Gemology*, 41(3), 234–244.
- Wang W., Scarratt K., Emmett J.L., Breeding C.M., Douthit T.R. (2006a). The effects of heat treatment on zircon inclusions in Madagascar sapphires. *Gems and Gemology*, 42(2), 134–150.
- Wang W., Gelb T., Dillon S. (2006b). LN: Coated pink diamonds. *Gems and Gemology*, 42(2), 162–163.
- Wang W., Scarratt K.V., Hyatt A., Shen A.H., Hall M. (2006c). Identification of “Chocolate Pearls” treated by Ballerina Pearl Co. *Gems and Gemology*, 42(4), 222–235.
- Watt G., Harris J.W., Harte B., Boyd S.R. (1994). A high-chromium corundum (ruby) inclusion in diamond from the São Luiz alluvial mine, Brazil. *Mineral.* 58, 490 - 493.
- Winotai P., Limsuwan P., Tang I.M., Limsuwan S. (2004). Quality enhancement of Vietnamese ruby by heat treatments. *AusG*, 22(2), 72–77.
- Wright F.E. (2014). Methods and instruments used in mineralogy. *AusG*, 6(2), 9-21.
- Xu J., Huang E., Lin J., Xu L.Y. (1995). Raman study at high pressure and the thermodynamic properties of corundum; application of Kieffer's model. *American Mineralogist*, 80(11-12), 1157-1165.
- Yager Y.G., Menzie W.D., Olson D.W. (2008). Weight of production of emeralds, rubies, sapphires, and tanzanite from 1995 through 2005. Open file Report 2008–1013, 9

APPENDIX A

Association of gemstone deposits to litho-stratigraphic units in Southern Kenya.

A table correlating geological formations in Southern Kenya, the rock types and the gemstones found in that region is provided below (Pohl and Nierdermayr, 1979, Simonet et al., 2000a).

Formation	Lithological association	Some of the Gemstones present
KASIGAU GROUP	amphibolites, metarkoses, calc-silicate rocks	Amethyst, hessonite, moonstone
KURASE GROUP		
Mugeno Formation	biotite-garnetkyanite-sillimanite-graphite, metalimestones (dominant) and quartzfeldspar-garnet gneisses	corundum, sapphire, spinel, pyropealmandine garnet, rhodolite
Mwatate Formation	Bandedgneisses, migmatites, biotite-garnet gneisses (dominant), kyanite-sillimanite quartzites and plagioclase amphibolites, metalimestones (minor),	tourmaline, rhodolite, tsavorite, corundum, color-change garnet, ruby, kyanite (?)
Mgama-Mindi Formation	marbles , (top) biotite-graphite gneisses,	korerupine, ruby, tourmaline, pyralspite garnet, rhodolite
idem (bottom)- Lualenyi Member	quartz-feldspar-garnet gneisses, graphite-sillimanite, gneisses with bands of granitoid marbles, amphibolites	ruby, tsavorite, korerupine and tourmaline
Mtongore Formation	banded gneisses, biotite-garnet gneisses, marbles, and quartz-feldspar-garnet gneisses	ruby, rhodolite, sapphire, corundum, korerupine, pyralspite garnet, diopside and tourmaline

APPENDIX B

Cause of Color Chart

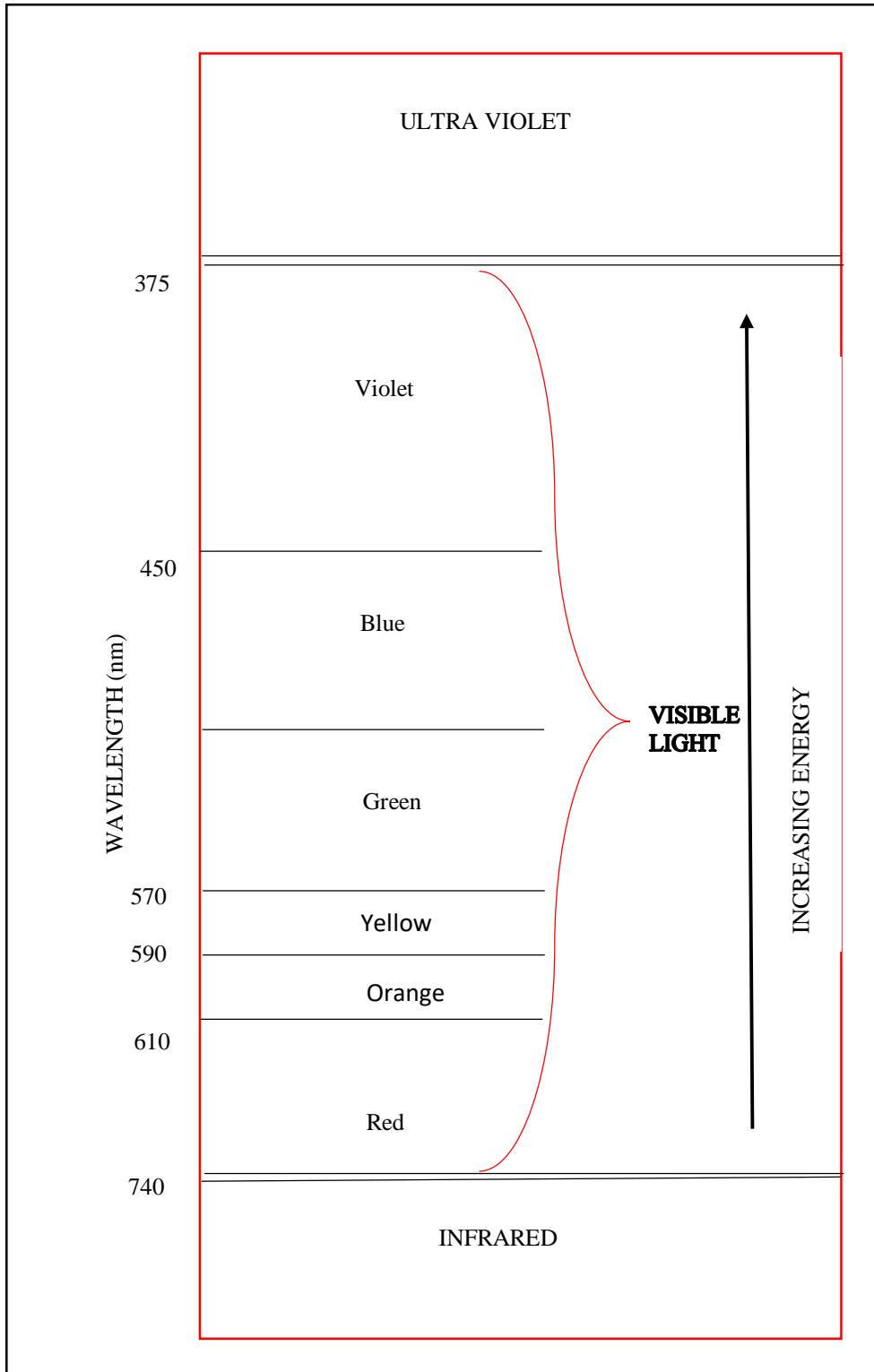
A table correlating the type of gem with the causes of its color (modified from Fritsch and Rossman, 1988; Jasinevicius, 2009)

Mineral	Color	Cause	Reference
Corundum	ruby red	octahedrally coordinated Cr³⁺ with some V³⁺ and Fe³⁺ in octahedral coordination	Fritsch and Rossman, 1988
	blue sapphire	Fe²⁺ O Ti⁴⁺ charge transfer	Fritsch and Rossman, 1988
	Purple	Fe²⁺ O Ti⁴⁺ charge transfer; with octahedrally coordinated Cr³⁺	Fritsch and Rossman, 1988
	orange-pink (padparadscha)	Still on debate; presence of Cr possible with other color centers, valence is debated	Fritsch and Rossman, 1988
	orange to brown	octahedrally coordinated Cr³⁺ with some Fe³⁺	Fritsch and Rossman, 1988
	Pink	octahedrally coordinated Cr³⁺	Fritsch and Rossman, 1988
	yellow	multiple possibilities relating to Fe (possible charge transfer or Fe-pairs)	Fritsch and Rossman, 1988
	Green	several possibilities involving either Fe and/or Cr³⁺	Fritsch and Rossman, 1988
Quartz	purple (amethyst)	A hole center created by presence of Fe and sometimes radiation	Paradise, 1982; Fritsch and Rossman, 1988
	yellow (citrine)	O²⁻ Fe³⁺ charge transfer	Fritsch and Rossman, 1988
	green (prasolite)	Fe²⁺	Paradise, 1982; Fritsch and Rossman, 1988).
	black (smoky)	hole center	Maschmeyer et al., 1980; Fritsch and Rossman, 1988
	pink (rosy) pink	Microinclusions	Goreva et al., 2001

APPENDIX C

The visible spectrum (Raman Spectroscopy utilizes the 514.5, 532nm (green spectrum) or the 785nm (red to infrared) laser)

All of the colors making up visible light corresponds to a specific energy range and wavelength.



APPENDIX D

Definitions

Mineralogy refers to the science of minerals or the branch of science that studies minerals (Bideaux et al., 2003, Kievlenko, 2003). The definition of mineralogy adopted in this study is the same as its literal definition.

Chemistry is the study of the composition and constitution of substances and the changes that they undergo as a consequence of alterations in the constitution of their molecules (Oxford dictionary). This definition is adopted for the study and restricted to specific gemstones.

Morphology is the scientific study of the structure and the form, without regard to its function. The definition of morphology adopted in this study was the study of the external form of the crystal gems (Channel, 2012).

Optimization is the design and operation of any process that makes it as good as possible or that gives the best possible results (Oxford dictionary). An Optimized thermal process adopted in this study was, the temperature at which the gem color changes in terms of permanence, brightness, deepness or to a totally different color.